CLOVIS-2 was carried out under a program of, and funded by, the European Space Agency (ESA) contract number: 4000133994/21/I-DT-lr

The **CERTAINTY** project has received funding from Horizon Europe programme under Grant Agreement No 101137680

Blinded by the lights

Visible reflectances and lightning imager data: measurements, modelling and information content

Angela Benedetti
Cristina Lupu
Philippe Lopez
Tobias Necker
Samuel Quesada-Ruiz

Thanks to Volkan Firat, Alan Geer, Liam Steele, Peter Lean, Mohamed Dahoui, Marco Matricardi, Josef Schröttle, Robin Hogan, Paolo Andreozzi, James Hocking, Christina Stumpf, Leonhard Scheck, Christina Köpken-Watts, Jérôme Vidot …

Objectives and goals for this lecture

1. Brief introduction to the visible part of the spectrum
2. Developments required to enable visible reflectance assimilation (observation operator, observation pre-processing, etc)
3. Lessons learned from monitoring and preliminary impact when assimilating visible reflectance observations
4. Future directions for visible reflectance assimilation
5. Lightning assimilation

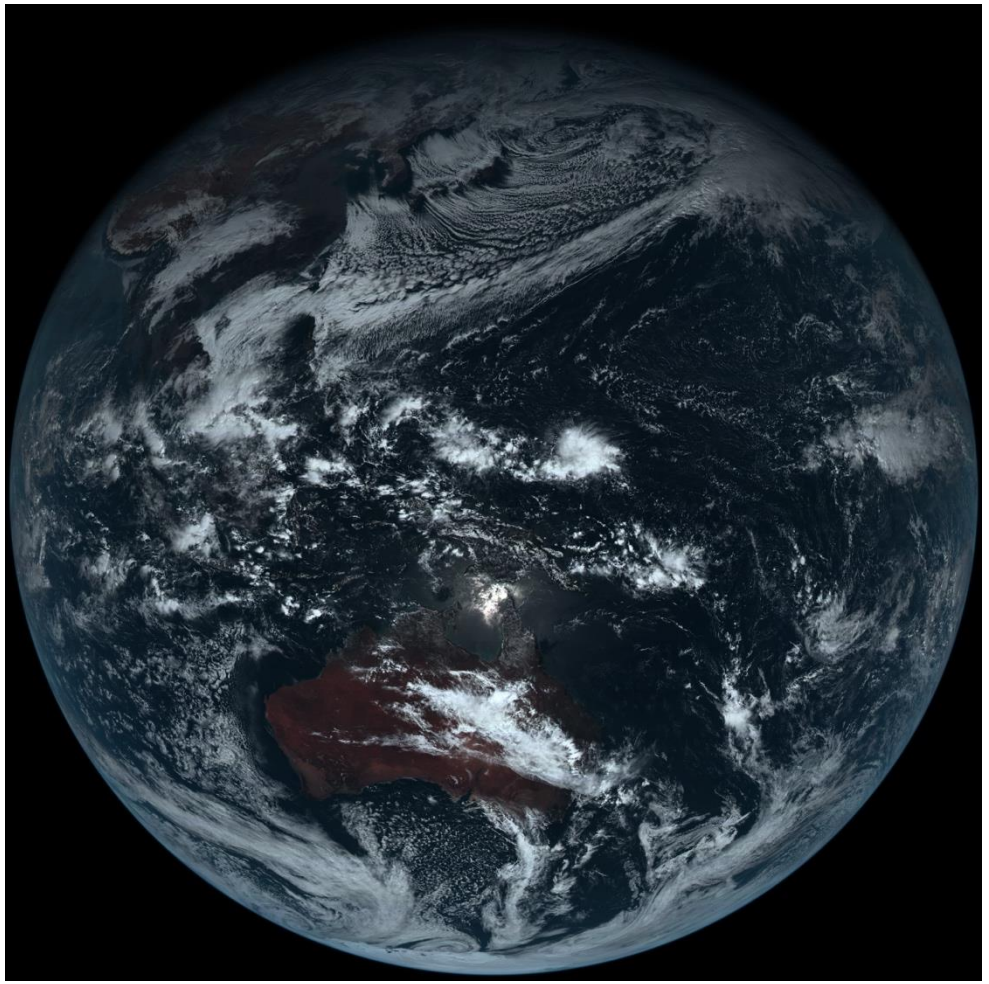

Continue to push boundaries of satellite observation exploitation

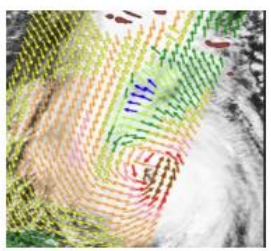
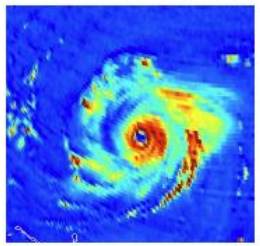
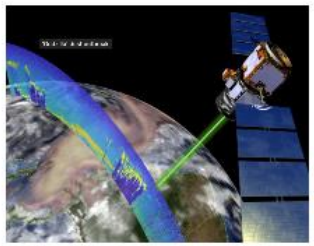
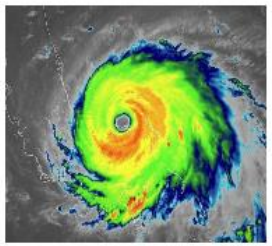


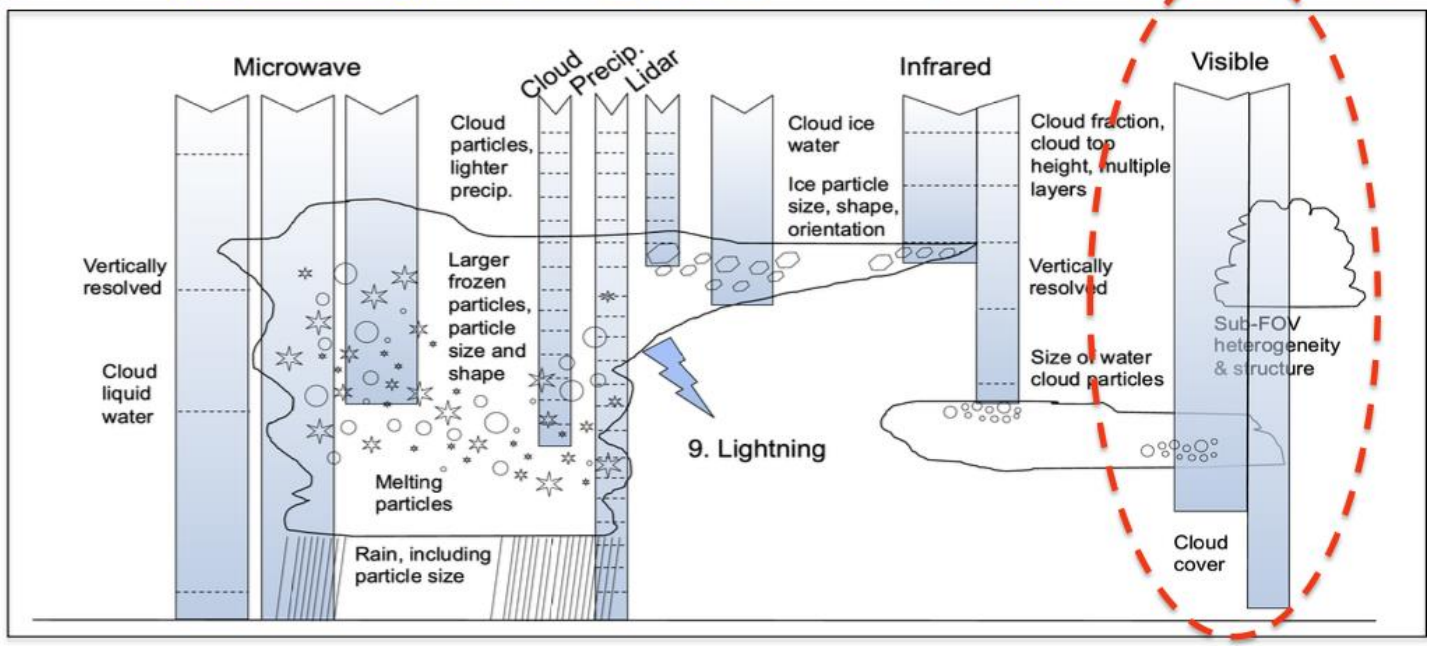

- Satellite observations make a major contribution to the Earth system data which are routinely assimilated into models to determine the initial conditions for weather forecasts.
- ECMWF has long led the way in assimilating humidity-, cloud-, and precipitation- sensitive microwave data for NWP (Geer & Bauer, 2011).
- Efforts continue to exploit information on cloud and precipitation in ‘all-sky’ conditions, using a broad range of available observations, including passive (e.g., IR) and active satellite instruments (e.g., EarthCARE lidar and Doppler radar).
- Visible observations can provide valuable additional information about clouds and aerosols, complementing what is available from IR and MW data (also considering new sensors).

This presentation highlights ECMWF’s developments to exploits visible radiance satellite observations for NWP.

1. Introduction

- Visible-spectrum characteristics and relevance for NWP
- RTTOV capabilities for modelling visible channels
- Visible observations from GEOS and LEO imagers
- Visible observation processing workflow at ECMWF

Visible radiance simulation is fundamentally different from infrared/microwave

- Visible radiation originates directly from sunlight
- Complex radiative transfer
  - reflection and multiple-scattering dominate the radiative transfer increasing computational demand of ***H***
  - sensitive to details of the optical properties of the atmospheric constituents, e.g., **cloud** and **aerosol particles**
  - need for accurate surface reflectivity models for land and ocean surfaces.
- Requires no weighting function (almost negligible emission/absorption)

Measured by the satellite

Our description of the atmosphere

$$L(\nu) = \int_0^{\infty} B(\nu, T(z)) \left[\frac{d\tau(\nu)}{dz} \right] dz + \text{Surface emission} + \text{Reflection/scattering} + \text{Cloud/rain contribution} + \ldots$$

Planck source term* depending on temperature of the atmosphere

Absorption in the atmosphere

Other contributions to the measured radiances

Important in IR range

Important in VIS range

Source: Tony McNally
ECMWF training material

Visible spectral bands in a nutshell

https://upload.wikimedia.org/wikipedia/commons/3/30/EM_spectrumrevised.png

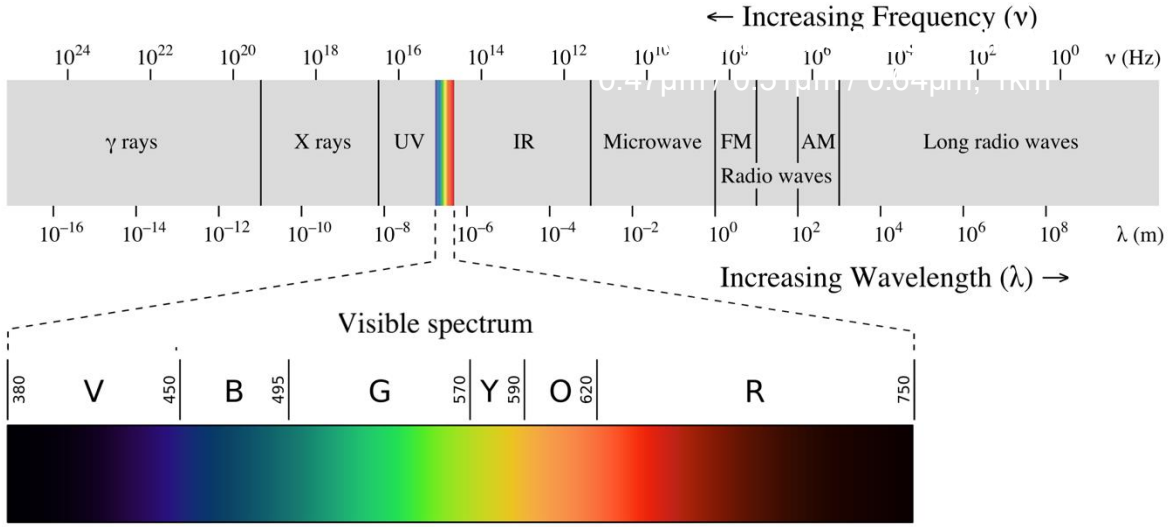

What now makes visible reflectance assimilation feasible?

- Availability of fast and accurate **forward observation operators**
- Sufficient **model cloud realism** – we can only assimilate what we can simulate
- **Exploitation of linearized moist physics -** TL/AD required to exploit information within 4D-Var.

Which spectral bands are we working on?

- **Visible** part of the spectrum, which ranges from about 300 – 800 nm (currently focusing: **655 nm**)
- **Near-infrared** part of the spectrum, which ranges from 800 - 2500 nm (currently focusing on **1600 nm**)

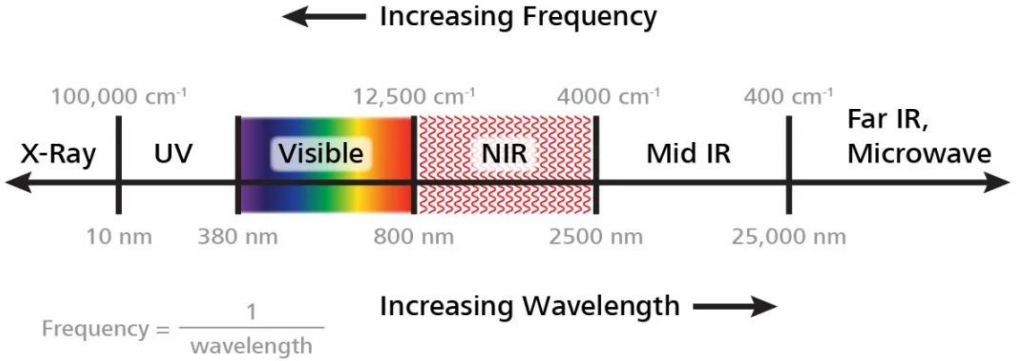

Image Credits: Metrohm AG

Cloud visible observation operator in RTTOV: **MFASIS-Cloud**

- DWD and HErZ play leading roles in the development and implementation of **MFASIS** (**M**ethod for **FA**st **S**atellite **I**mage **S**ynthesis, Scheck *et al.,* 2021) within the RTTOV NWP-SAF framework. At present, **clouds and aerosols are treated independently** (e.g., MFASIS-Cloud and MFASIS-Aerosol)
  - Fast and accurate approximation of 1D RT 'Discrete Ordinate Method' solution for visible in the presence of clouds, suitable for DA and model evaluation
  - Fast and memory-efficient forward operator based on neural network (**NN**) approach with limited set of input parameters per atmospheric model column (RTTOV-13.2 and later versions; trained on DOM)
    - First MFASIS version was based on lookup tables **LUT** (available with RTTOV-13, discontinued with RTTOV-14.0)
  - Estimate RT solution for the reflectance of complex atmospheric profile using feed-forward neural network with a reduced set of input variables (~ several 1000 parameters); The input layer consists of 16 normalised input parameters including liquid/ice/mixed optical depth, liquid/ice/mixed effective particle radii, surface and cloud top pressure solar, satellite and scattering angles.

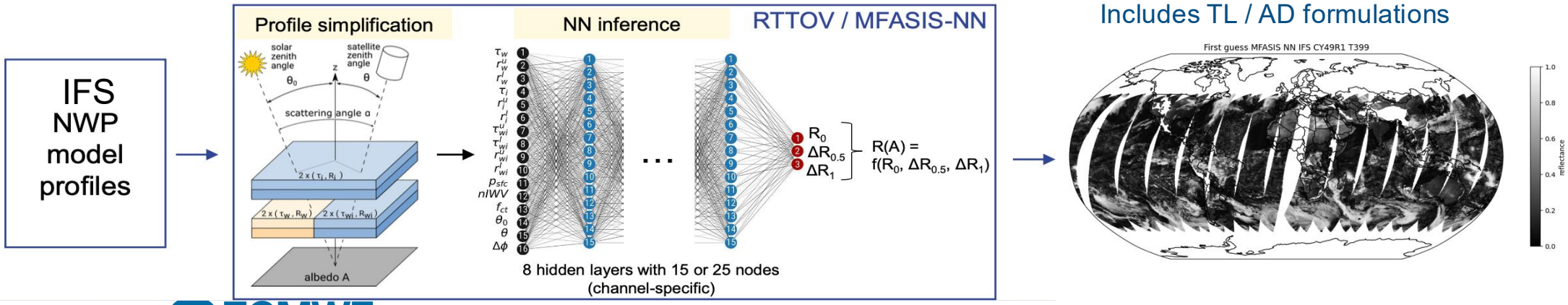

Source: DWD / Leonhard Scheck

Aerosol visible observation operator in RTTOV: **MFASIS-Aerosol**

- A prototype based on CAMS aerosols; MFASIS-Aerosol version is integrated within RTTOV-14.1
  - Can we generate reflectances for arbitrary combinations of many aerosol species with one NN and still have sufficiently small errors? Species A may be above species B or vice-versa…
  - Same strategy as for clouds: the aerosol content from the original profile is represented in a simplified profile by concentrating the 9 CAMS aerosol species defined in RTTOV (i.e., sea salt, desert dust, organic matter, black carbon, sulphate) into two distinct layers.
  - This approach captures boundary-layer aerosols and a middle-to-upper tropospheric plume while preserving the total vertical integral of the aerosol loading.
  - Future re-training of MFASIS-Aerosols will make use of the 16 CAMS-species.

Includes TL / AD formulations

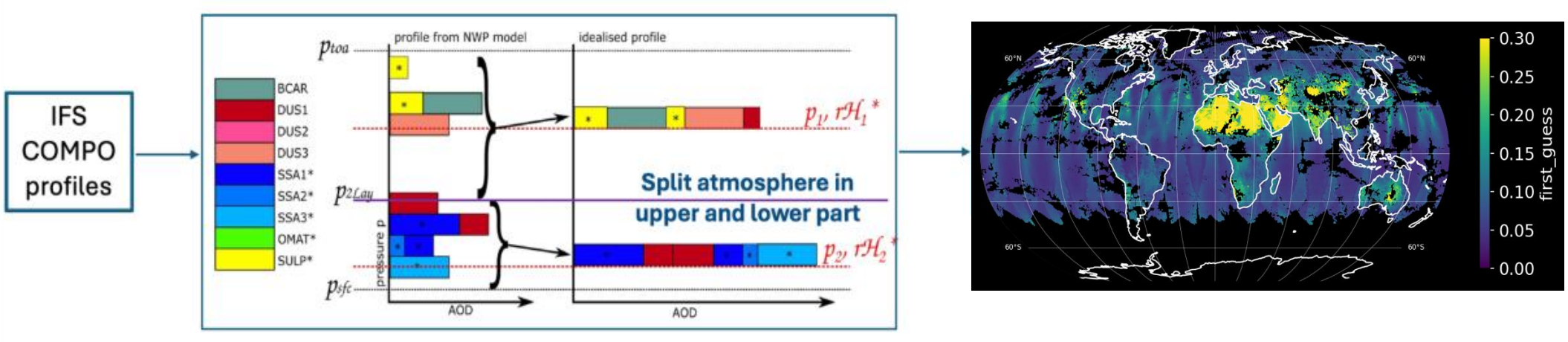

Source: DWD / Leonhard Scheck

RTTOV / Surface reflectance

- BRDF (Bidirectional Reflectance Distribution Function) model for VIS wavelengths
  - **Sea** – RTTOV's internal surface reflectance scheme, based on the Elfouhaily et al., 1997.
  - **Land** – atlases are provided (Vidot et al., 2018)
    - Global atlas of mean monthly land BRDF values for 2007 at 0.1 degree is used to specify **snow-free land** reflectances that are more realistic than RTTOV's default fixed value.

BRDF mask and quality index (January 2007)

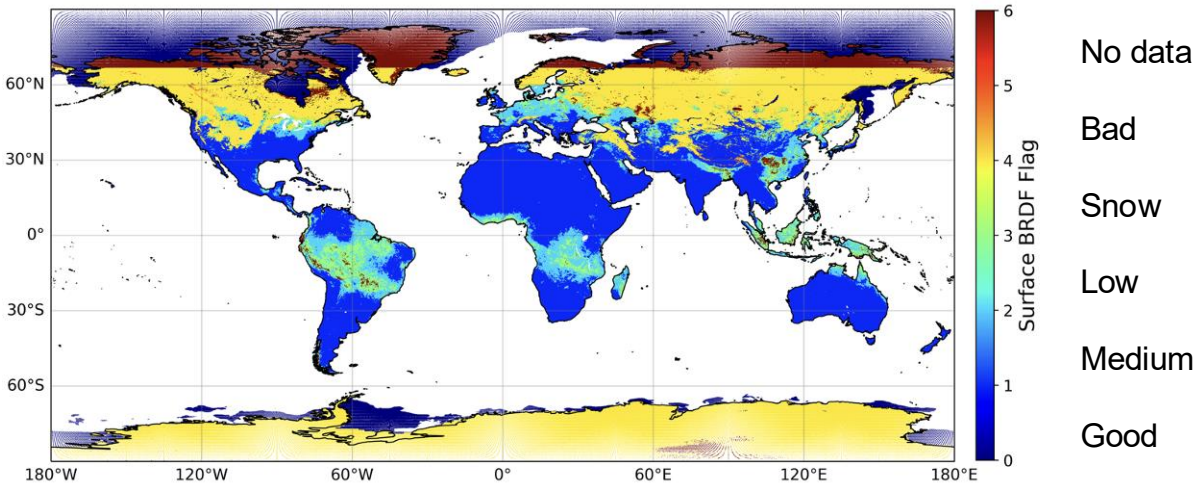

- A mask is provided for each of the BRDF datum providing information on the surface type (water, snow-free land with three levels of retrieval quality, snow with two levels of retrieval quality, and no data).
- Satellite visible data used for defining the surface BRDF values, are not available over regions affected either by permanent polar night or by permanent cloud cover.
- Account for the atlas for the month which corresponds to the current simulated imagery forecast time step.

Reflectance parametrization over **snow-covered land** in the IFS

- The reflectance over snow-covered land depends on the **skin temperature** and on the **high-vegetation fractional cover** (Lopez et al., 2022, Tech Memo 892)

$$R_\lambda^{snow} = \max\left\{R_{max}^{snow} - \left[\max\left(\frac{T_{skin} - 268.15}{12}, 0\right)\right]^2, R_{min}^{snow}\right\}$$

where $R_{max}^{snow} = 0.85 - 0.45 f_{hveg}$ and $R_{min}^{snow} = 0.50 - 0.25 f_{hveg}$

- The overall reflectance of a given snow-affected land point:

$$R_\lambda = R_\lambda^{land} + (R_\lambda^{snow} - R_\lambda^{land}) \times f_{snow}$$

R_λ^{land} reflectance of snow-free land (set to 0.25)

$f_{snow} = \min(10000 \frac{h_{snow}}{\rho_{snow}}, 1)$ snow fractional cover (0-1), calculated using the snow depth (in metres of water equivalent) and the snow density (kg/m^3)

and includes:
- the observed non-linear decrease of surface snow albedo with increasing temperature
- the observed reduction of snow-pack reflectance in regions with high vegetation

- Solar radiances over land will be modelled more accurately in winter months.

Visible reflectances observations from LEO imagers

- **Ocean and Land Colour Instrument (OLCI)** measures the reflectance of sunlight from Earth's surface/atmosphere in 21 spectral bands at a resolution of 300 metres

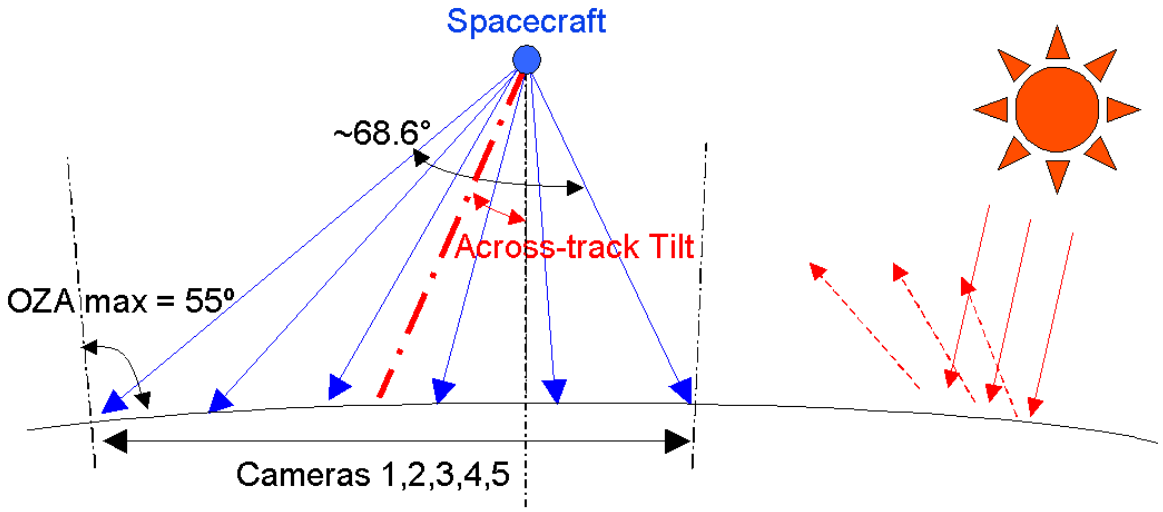

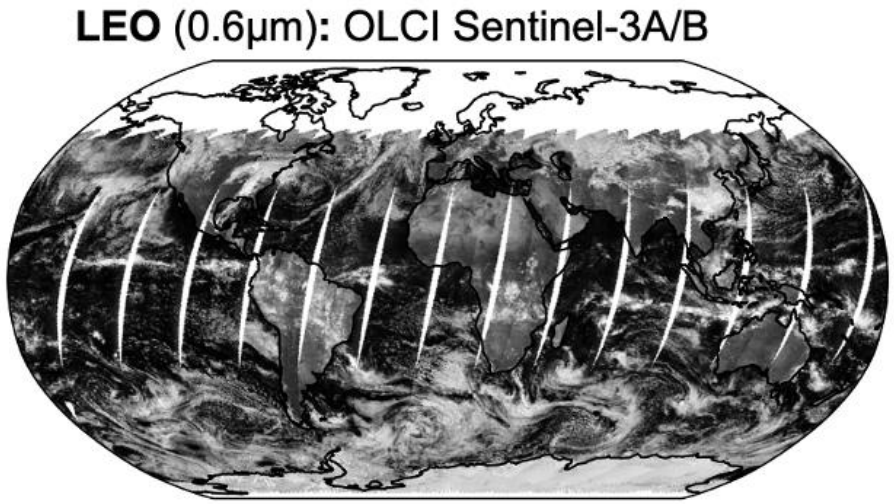

Schematic View of the OLCI Field of View (see https://sentiwiki.copernicus.eu/web/s3-olci-instrument)

Visible reflectances observations from GEOS imagers

- ECMWF aims to exploit high-resolution visible reflectances from all operational geostationary imagers
  - provide cloud information at much higher spatial and temporal resolutions than MW observations.

Visible channels by instrument

Channels (µm)	SEVIRI	ABI	AHI	FCI	OLCI
1	0.635	0.47	0.47	0.444	0.655
2	0.81	0.64	0.51	0.510	0.865
3	1.64	0.86	0.64	0.640	
4		1.37	0.86	0.865	
5		1.6	1.60	0.914	
6		2.2	2.30	1.380	
7				1.610	
8				2.250	

GEOS (0.6µm): ABI, FCI, SEVIRI, AHI

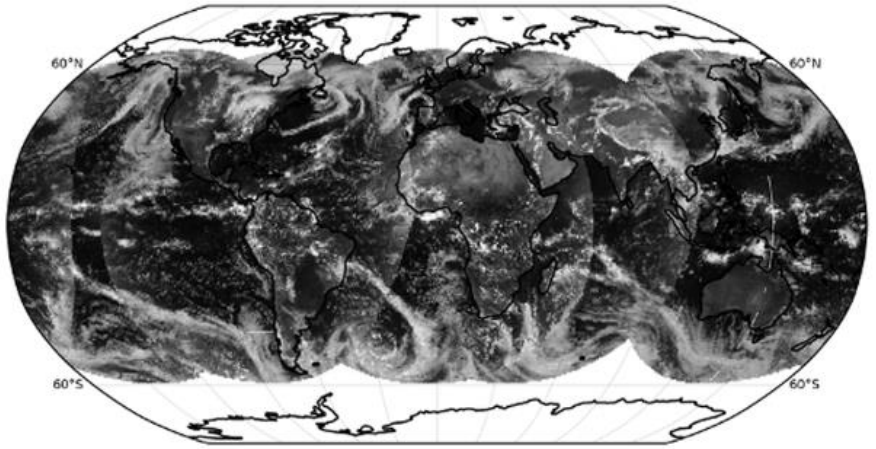

Visible observation processing workflow

- Build a bespoke data flow for pre-processing GEOS/LEO visible observations obtained from EUMETCast

NRT VIS data acquisition from EUMETCast

Pre-processing in local BUFR format

Superob reflectances

ODB format

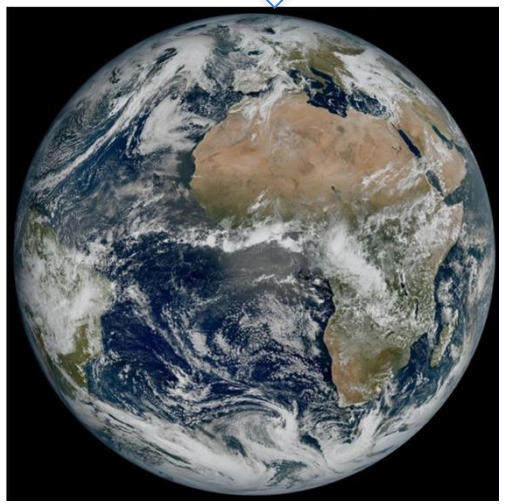

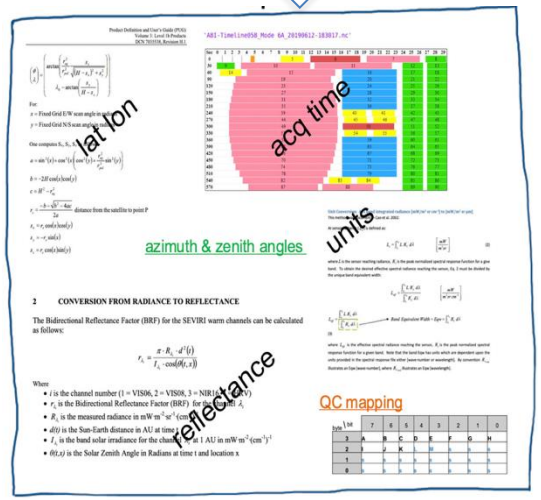

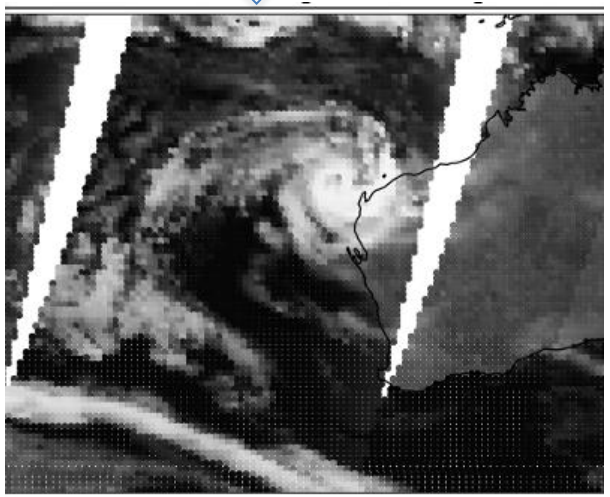

ODB is in-house data storage software to allow the 4D-Var system within IFS to store and access data.

2. Monitoring visible reflectances (clouds and aerosols)

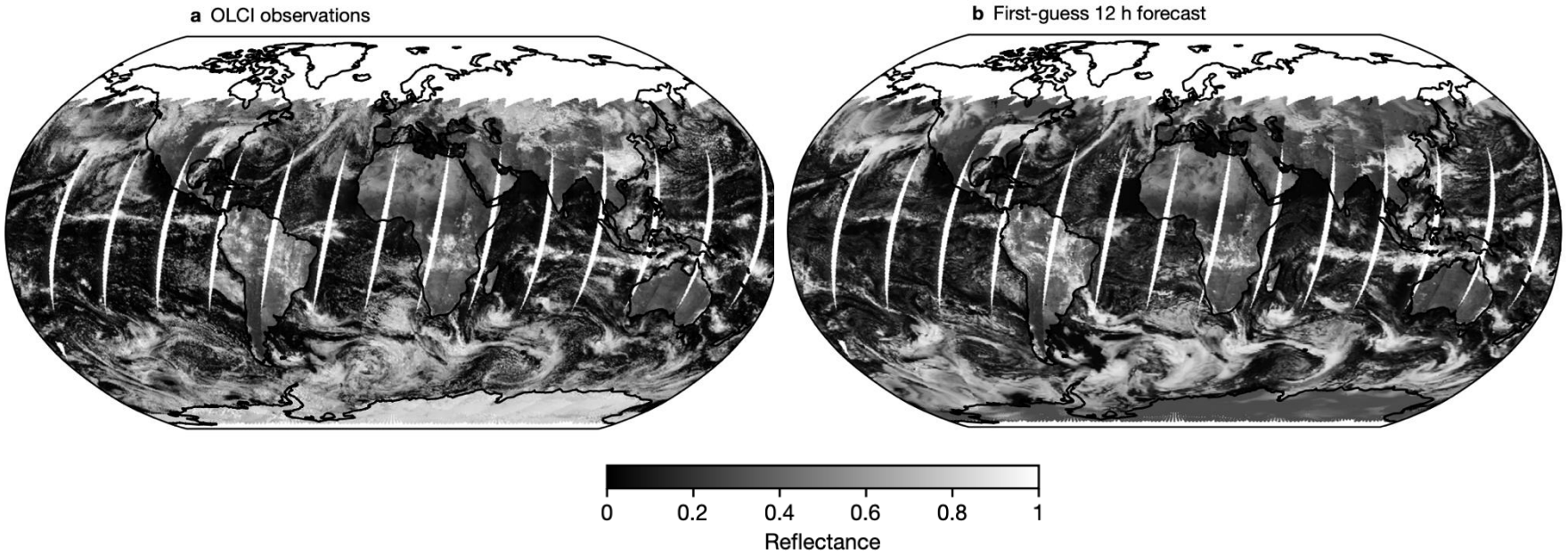

Comparison of mean simulated and observed MET-10 SEVIRI reflectances

Observation

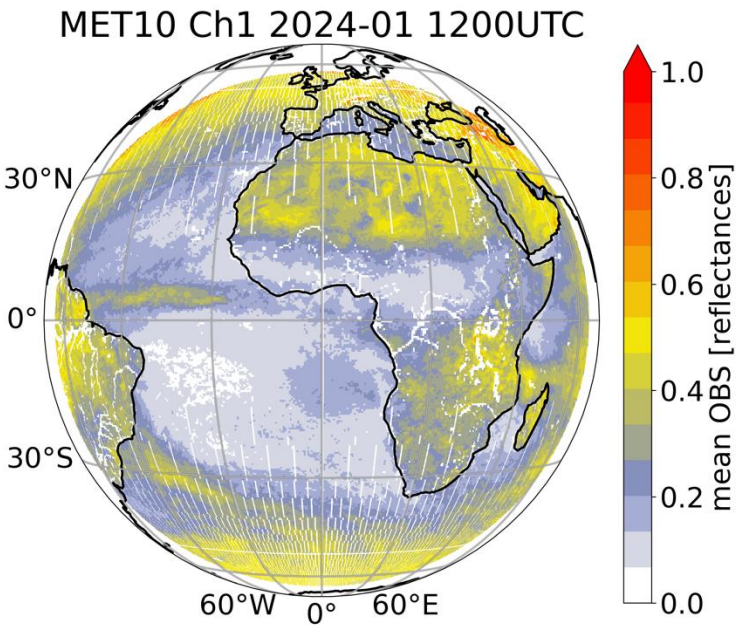

Simulation

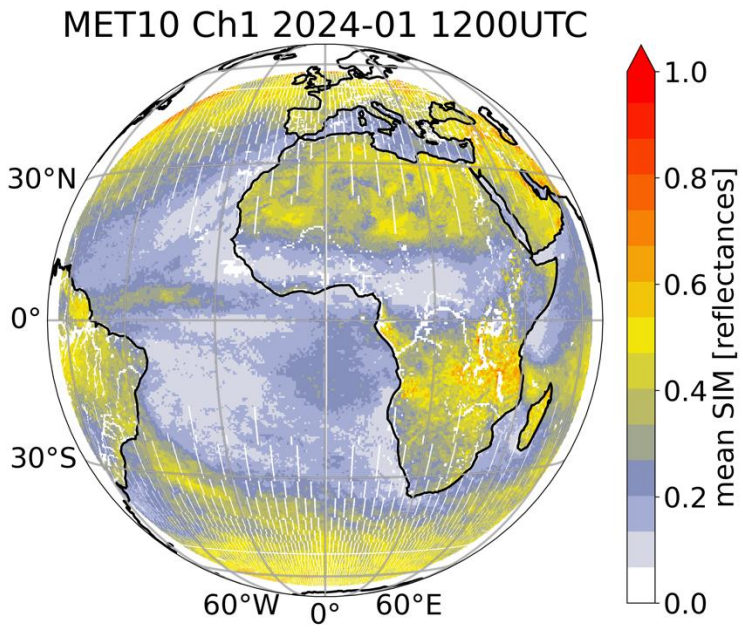

Average departure maps (O-B)

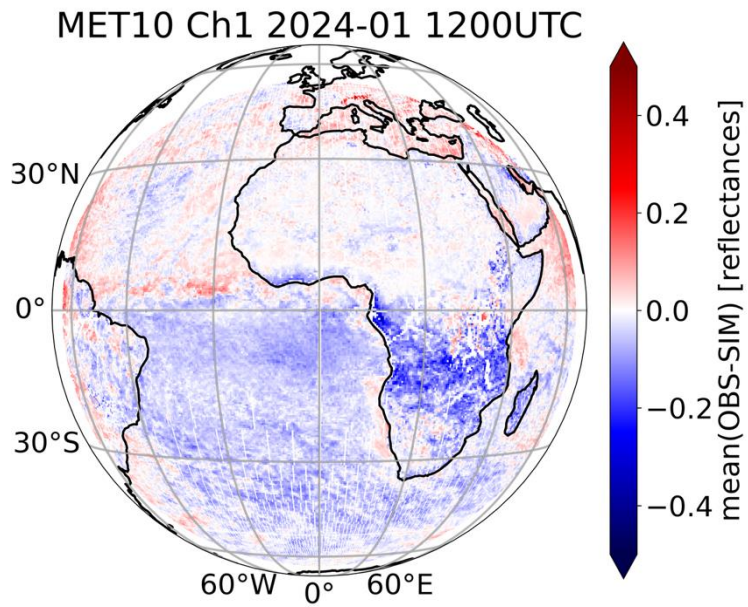

All data – no quality control

- Key parameter used for monitoring is the difference between observations (*O*) and the model background (*B*), or *O-B,* expressed in units of reflectance and before any bias correction is applied.
- Biases can be the results of radiative transfer deficiencies and/or IFS modelling errors, reflectances (calibration).

Showcasing the importance of observation screening for SEVIRI 640nm

Average departure maps (O-B)

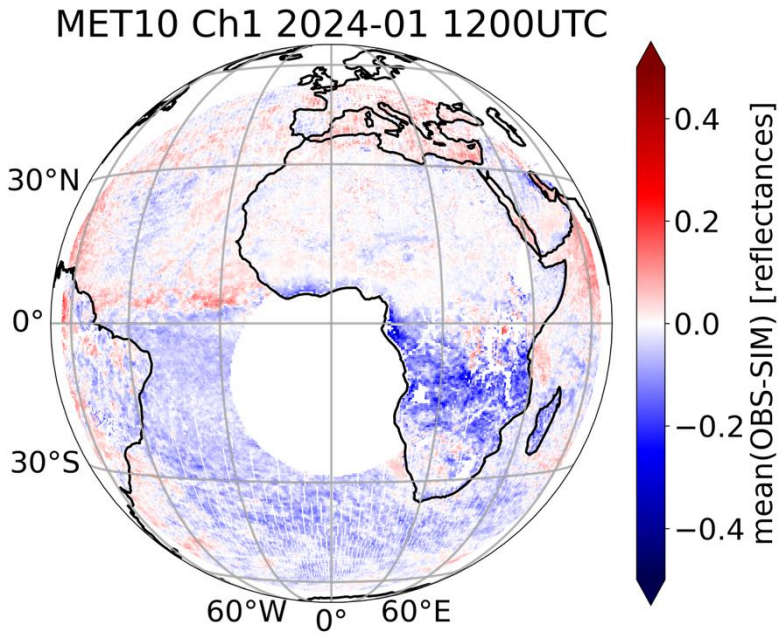

Reflectance frequency histogram

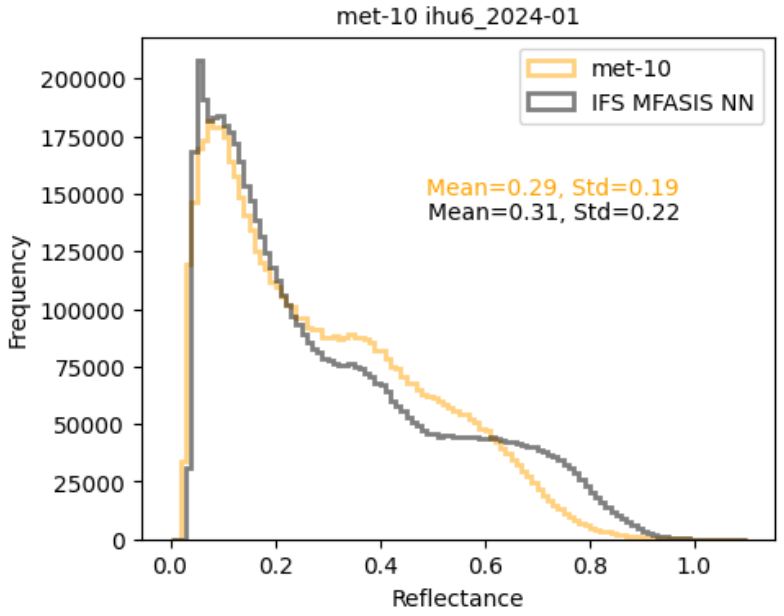

O-B histogram

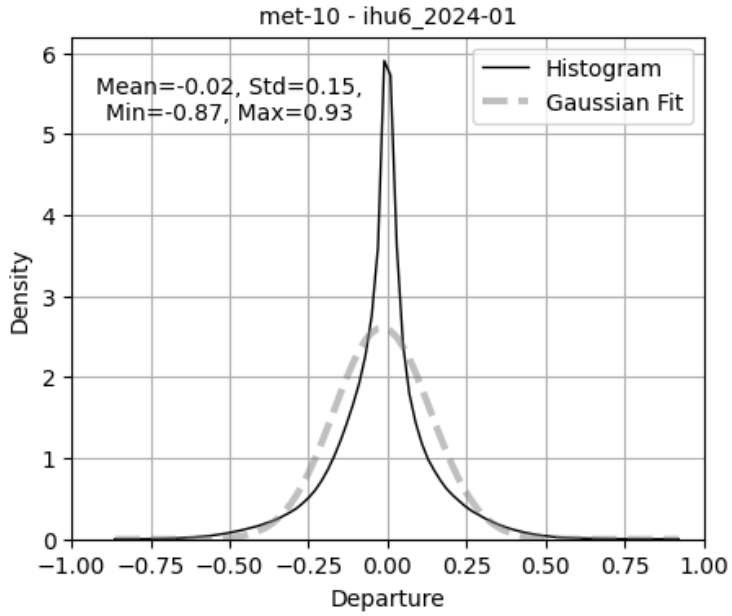

Quality controls checks applied: excluded sun zenith angle (>74, nighttime conditions); removed sunglint from sea surface (glint angle<40); sea-ice and heterogeneous surfaces avoided (coasts, lake borders, small lakes); model orography (>1500m, to avoid misinterpretation of snow as clouds), BRDF atlas used over snow-free land.

Showcasing the importance of SEVIRI 640 nm reliable calibration

Average departure maps (O-B)

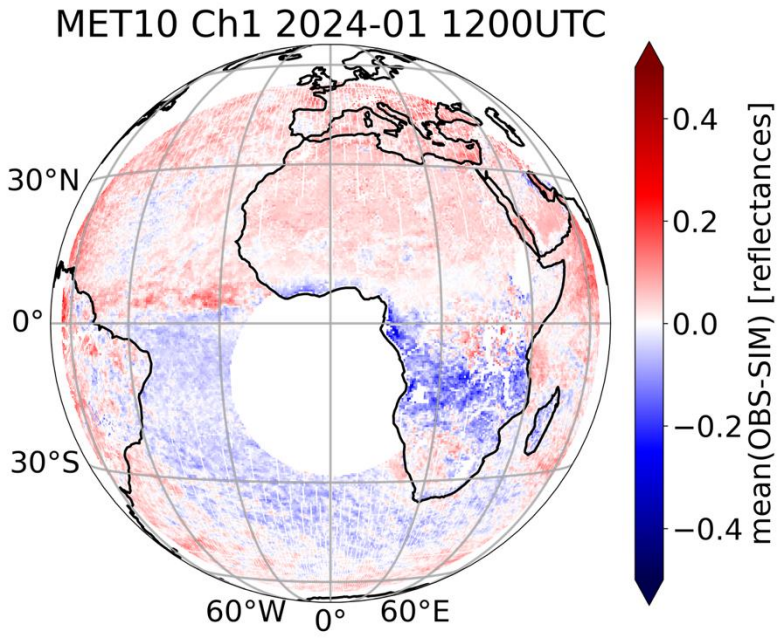

Reflectance frequency histogram

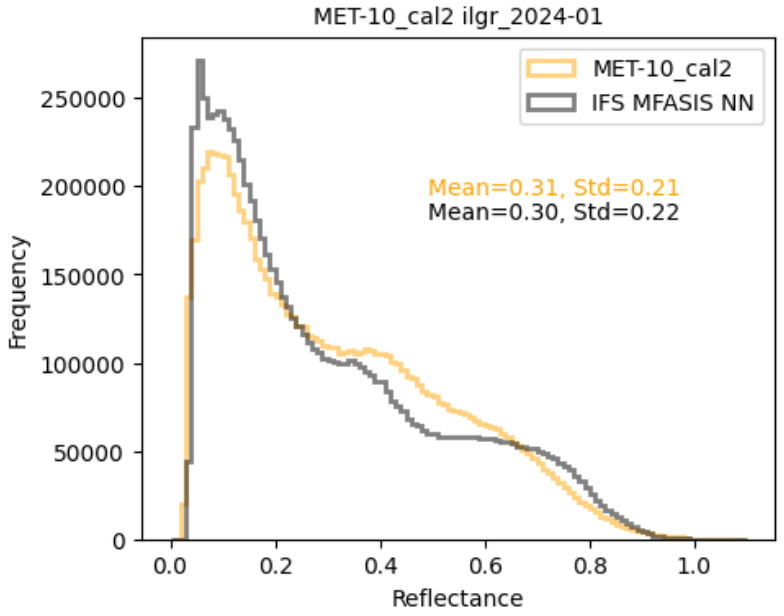

O-B histogram

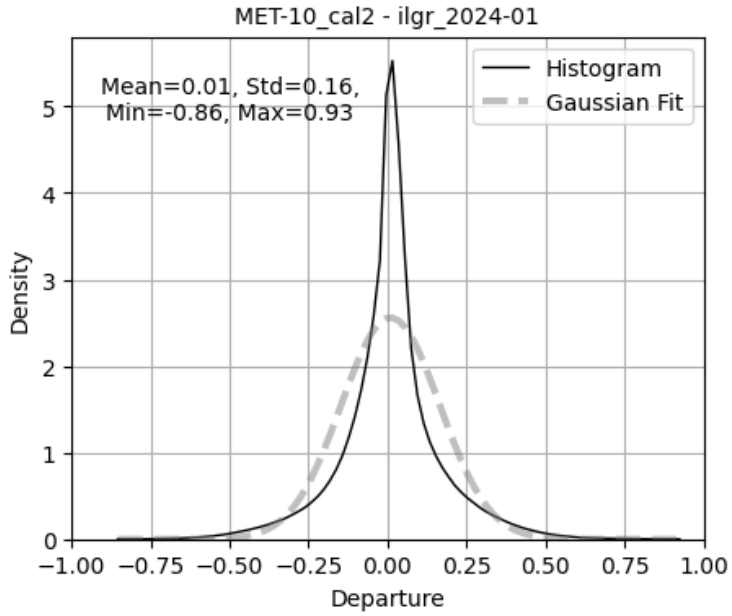

Operational calibrations of SEVIRI's warm channels were systematically darker → New EUMETSAT vicarious desert calibration method (MICMICS)→significant change, an 8.8% increase in the calibration gain for the Met-10 640 nm channel.

Showcasing the importance of BRDF atlas for RTTOV

Average departure maps (O-B) & Land reflectance histograms

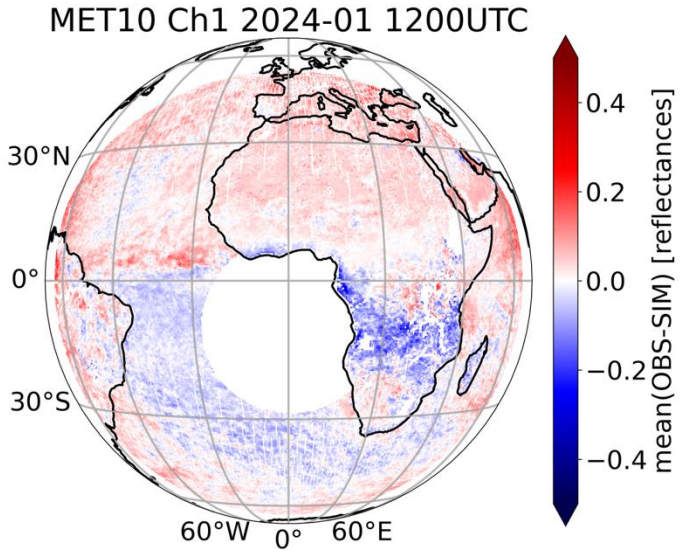

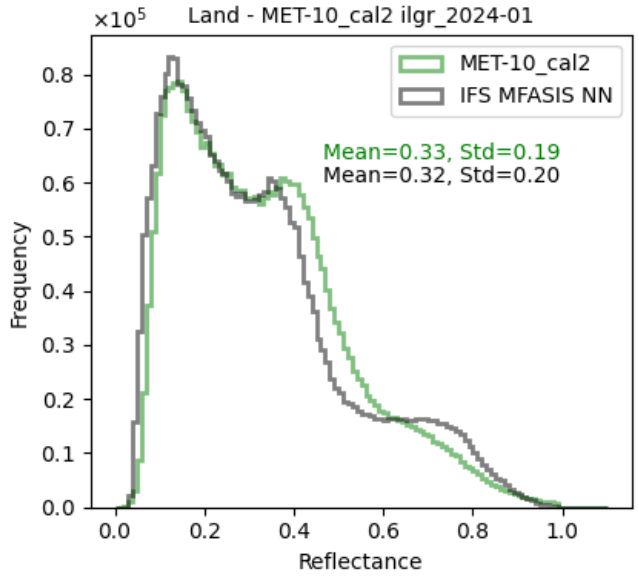

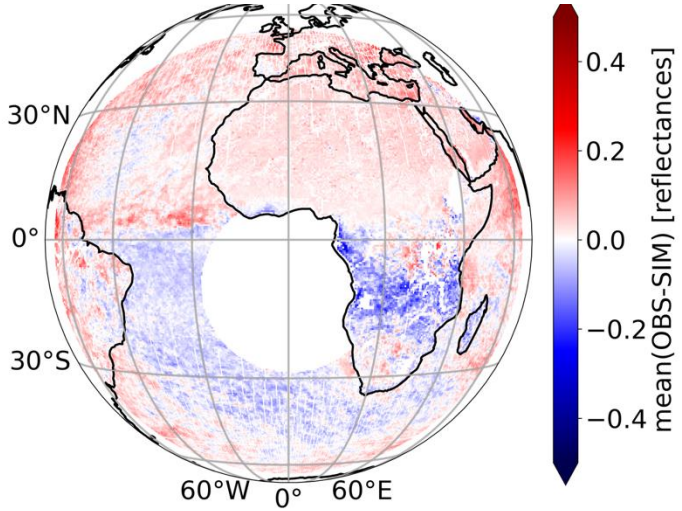

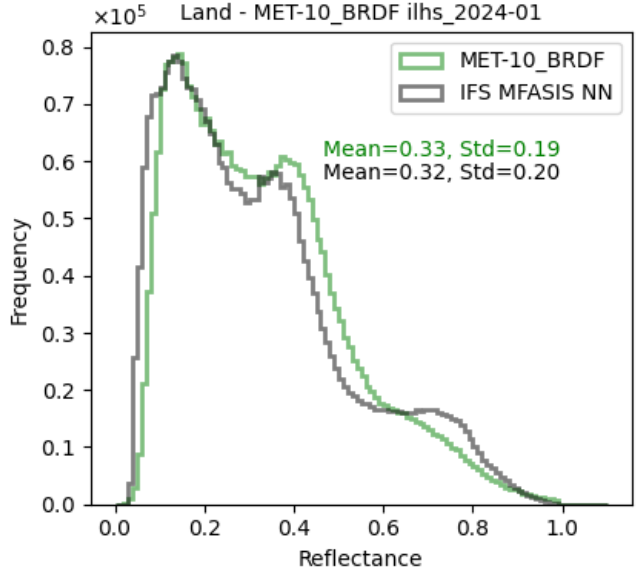

BRDF mask and quality index

January 2007, MODIS collection 5

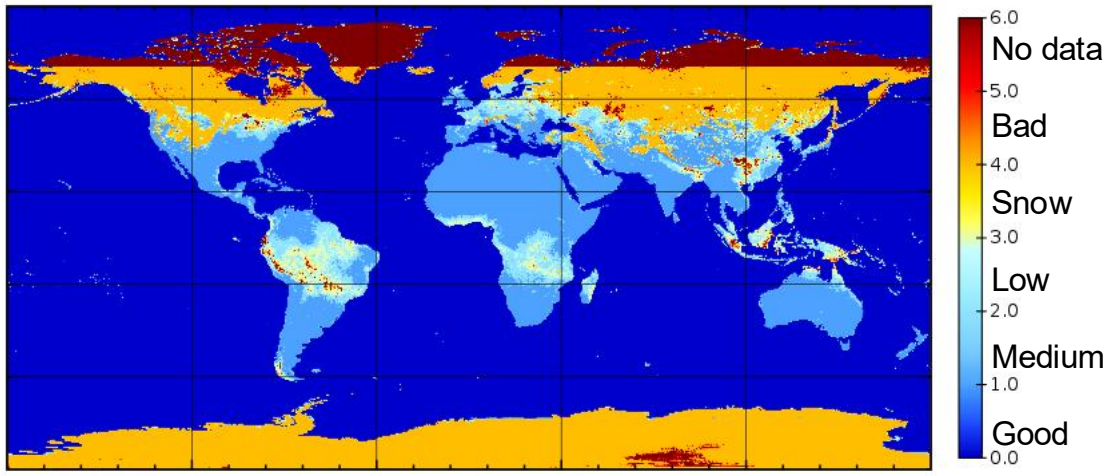

January 2024, MODIS collection 6

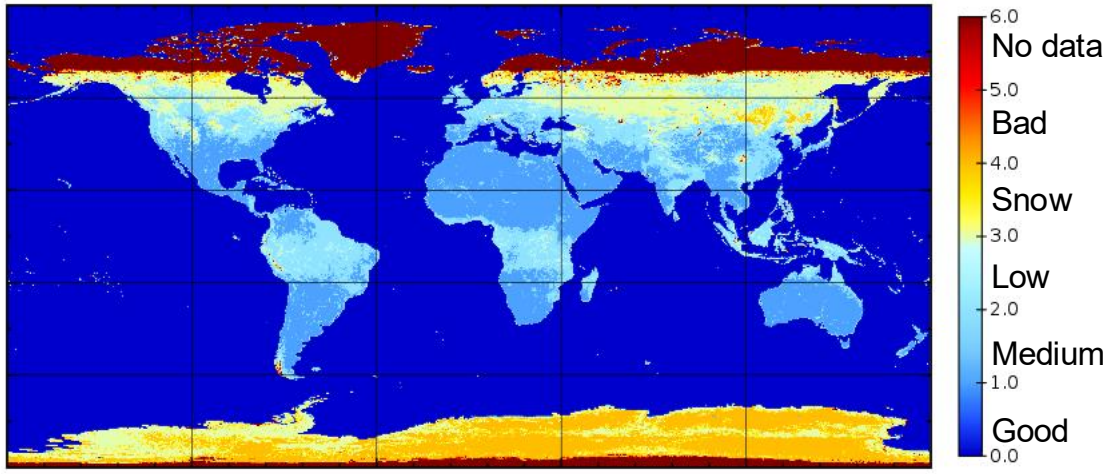

Showcasing the importance of observation screening for OLCI visible 655nm

Average departure maps (O-B)

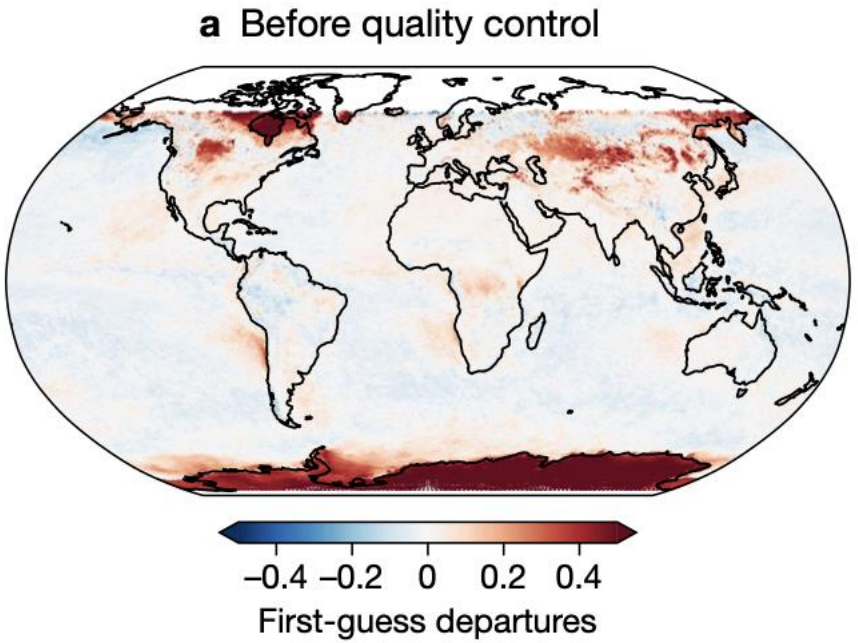

All data – no quality control (QC)

Reflectance frequency histogram

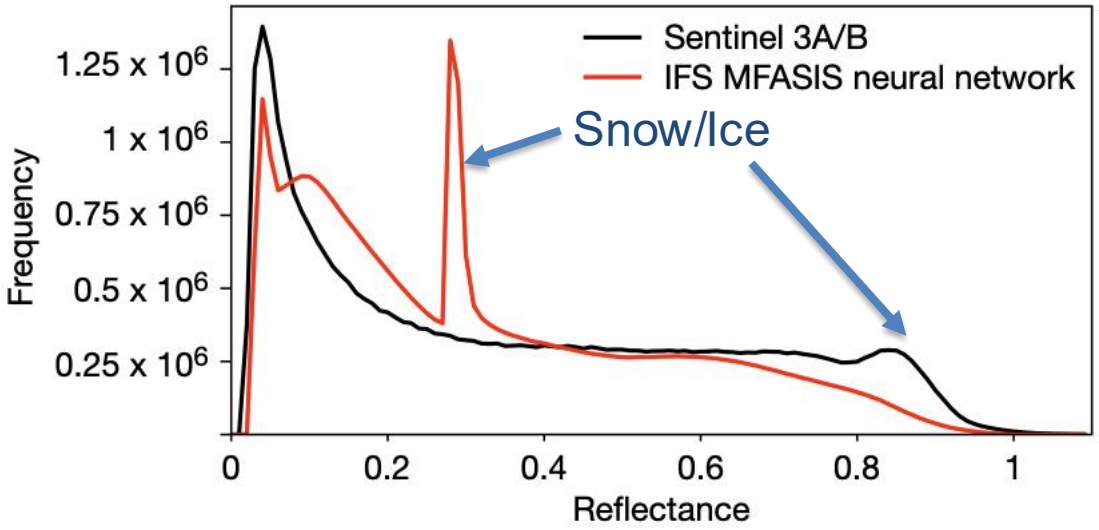

- Need for careful data screening, especially for areas affected by ice, snow, or observations at extreme sun or satellite angle.

Showcasing the importance of observation screening for OLCI visible 655nm

Average departure maps (O-B)

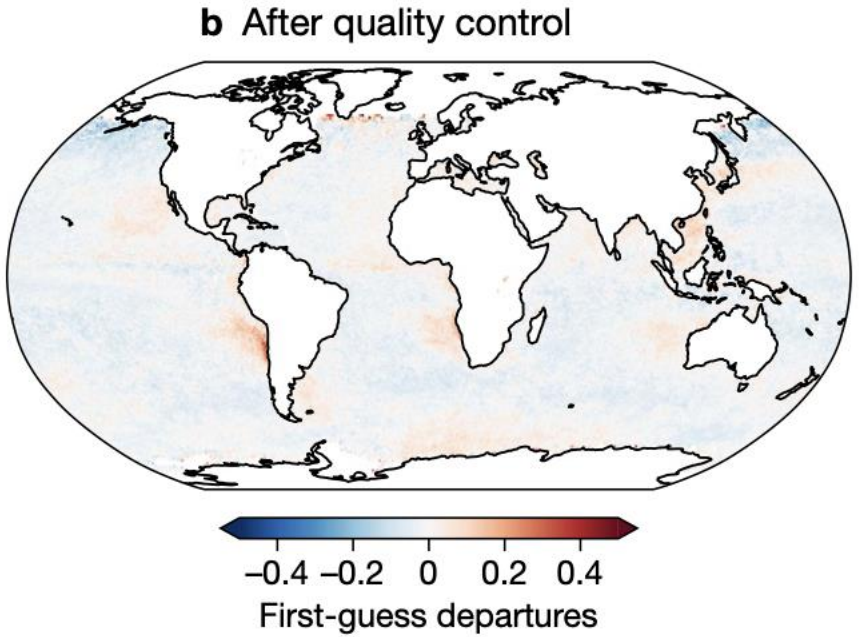

Reflectance frequency histogram

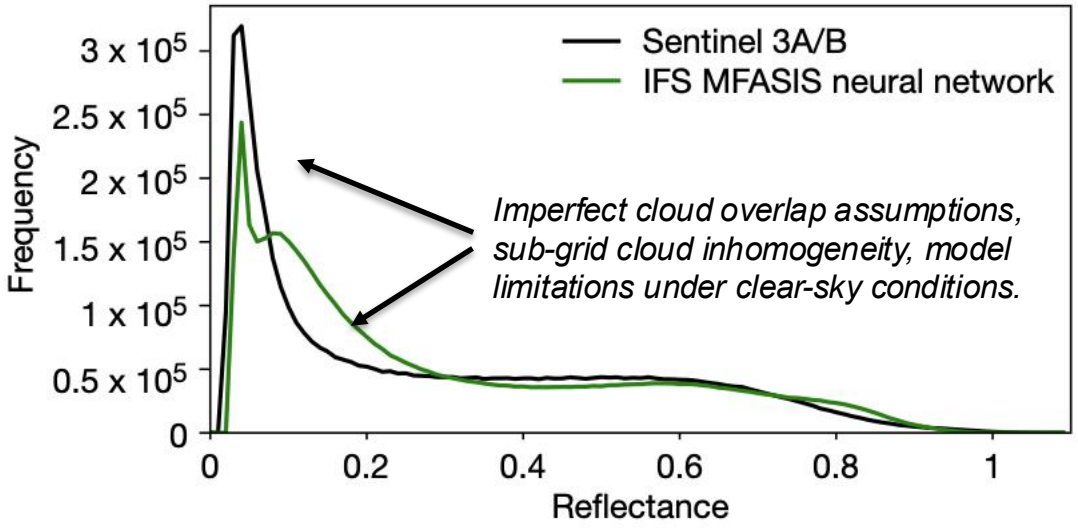

Active data - QC flags Sea-ice, solar/satellite zenith angles, sun glint, orography **removed**

Ocean only data provides good agreement between OLCI and IFS

Instrument dependent bias: OLCI/S3A brighter than OLCI/S3B

Time series of daily mean (O-B) departures (All data)

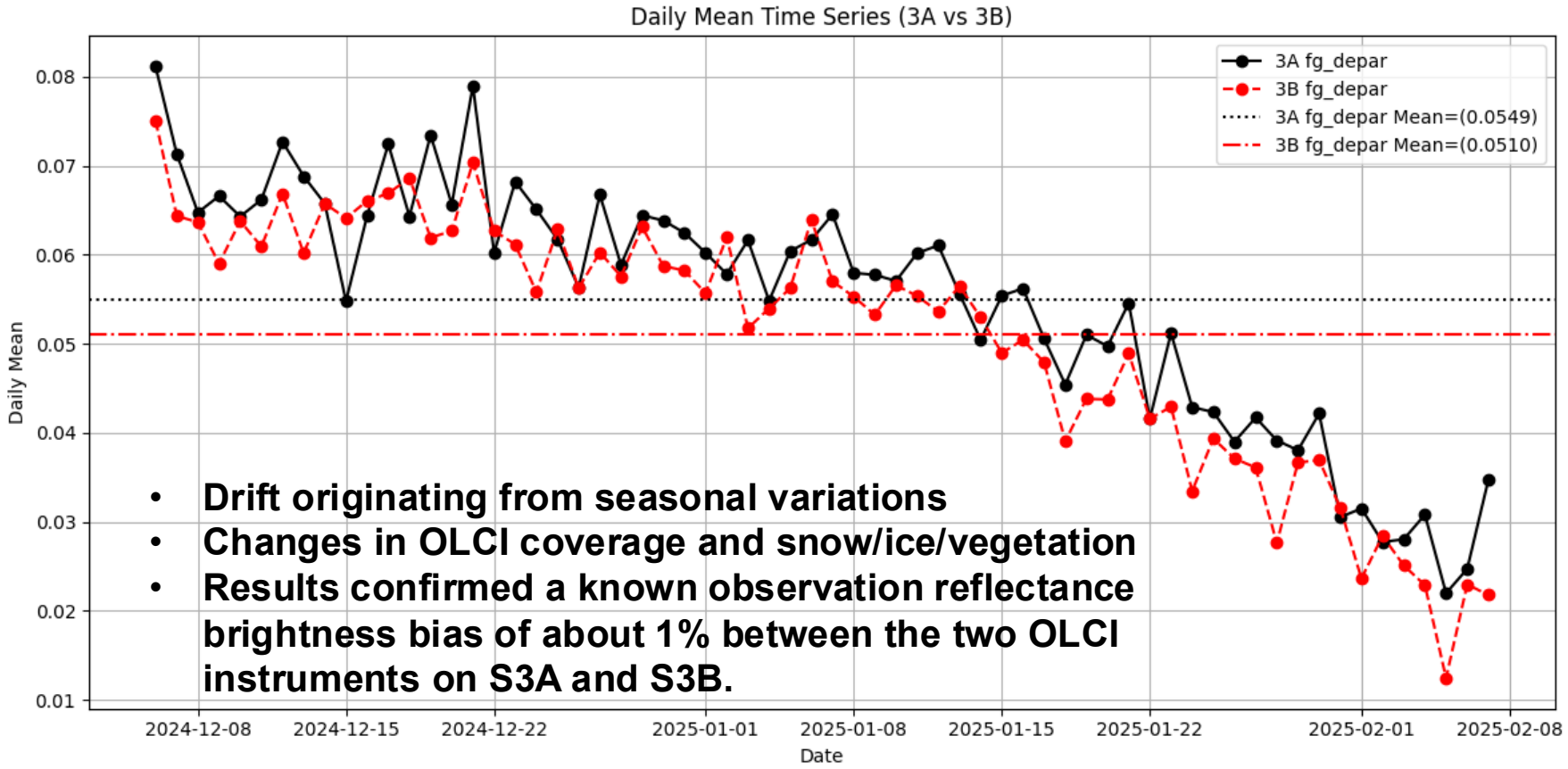

- **Drift originating from seasonal variations**
- **Changes in OLCI coverage and snow/ice/vegetation**
- **Results confirmed a known observation reflectance brightness bias of about 1% between the two OLCI instruments on S3A and S3B.**

Difference in brightness

OLCI/S3A

OLCI/S3B

Surface type dependent bias: Land vs Sea

Time series of daily mean (O-B) departures (Active data only)

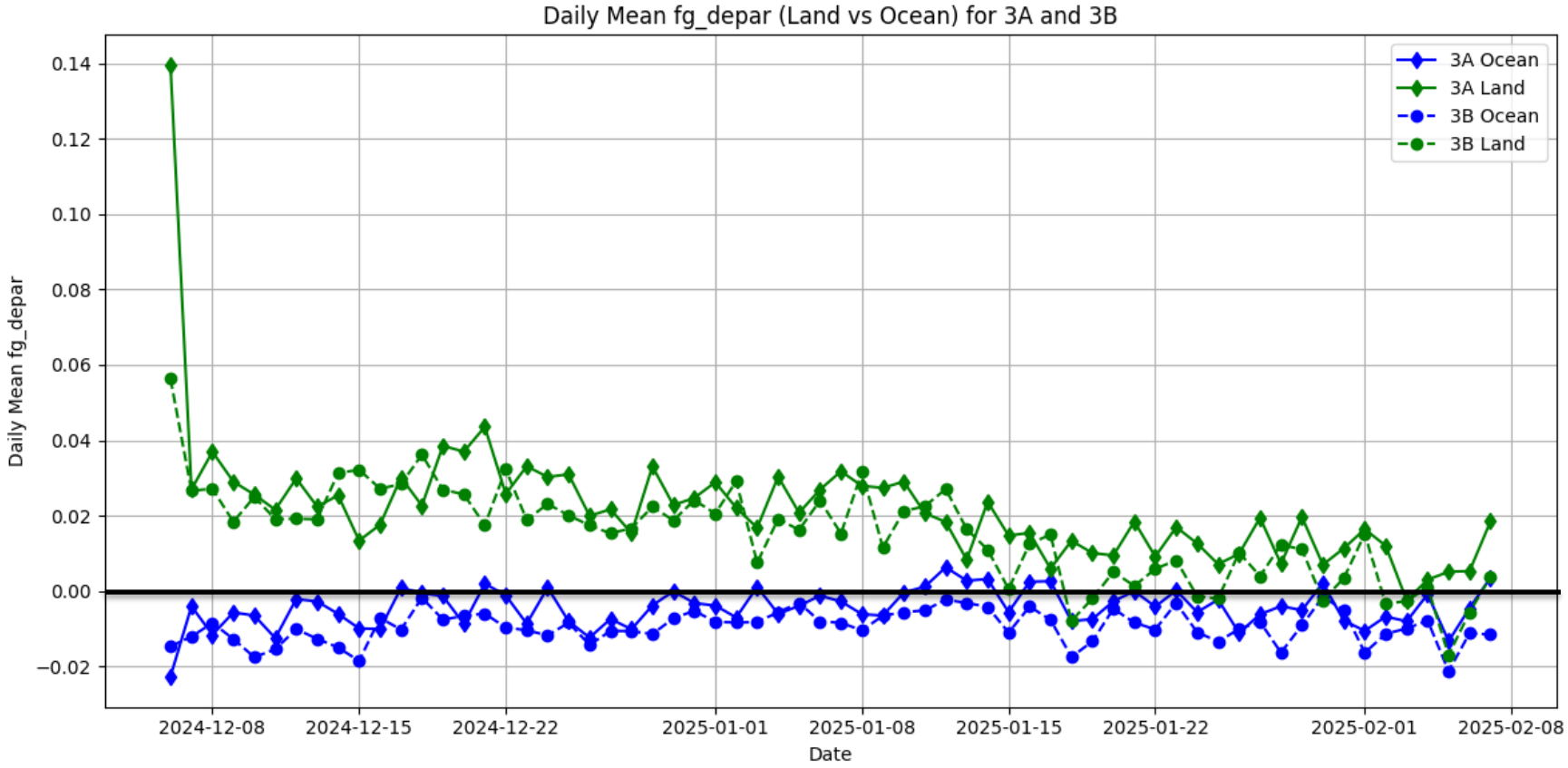

- Model and observation differences: systematic differences exist and must be minimized through improved model representation and observation operators.
- Model or observation bias?

IFS darker over land

IFS brighter over sea

Model and visible observations intercomparisons

May 2025

Departure maps (O-B): Active, **OLCI** (0.6µm)

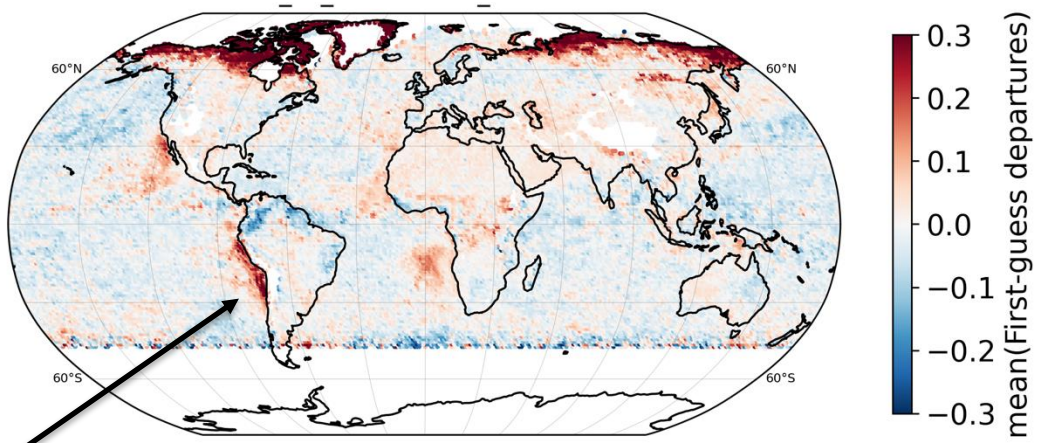

Systematic IFS biases

Departure maps (O-B): Active, **GEOS** (0.6µm)

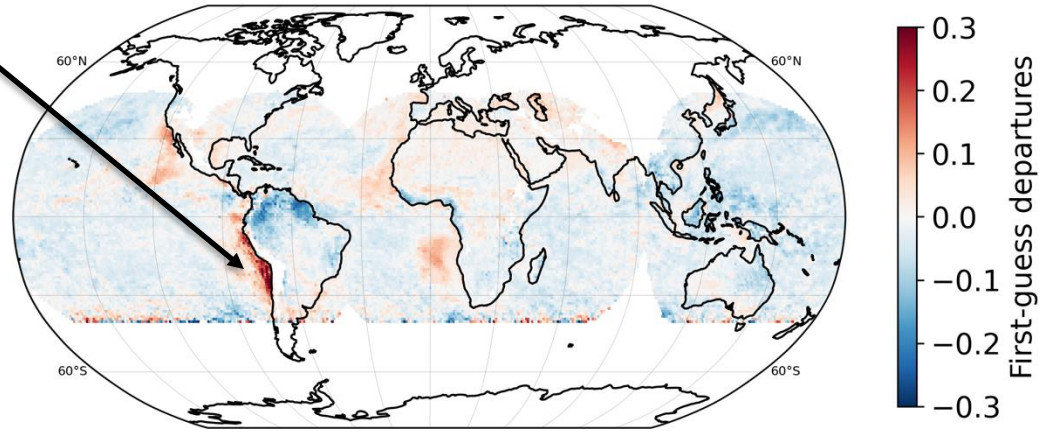

- Consistent spatial patterns emerged, particularly notable over maritime cloud regions, indicative of **persistent IFS model biases** rather than instrument-specific issues.

Model and visible observation intercomparisons

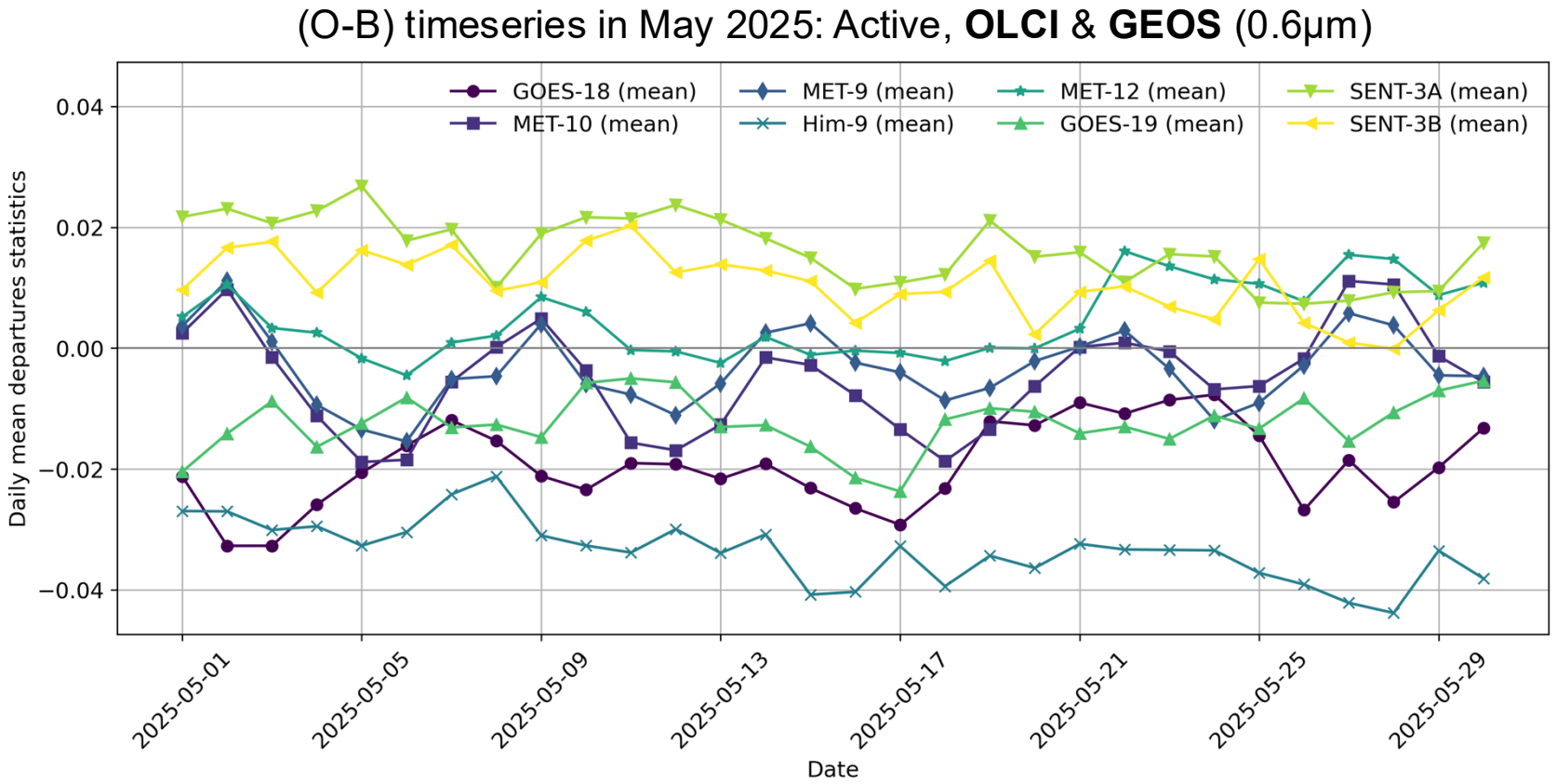

- Results confirmed a known observation reflectance bias of about 1% between the two OLCI on S3A and S3B.
- NWP powerful tool for data QC, Cal/Val and to ensure the reliability of both satellite observations and model performance.

What about aerosols?

Aerosol visible reflectances monitoring/assimilation requires careful treatment of cloud sensitivity, three approaches identified:

- Apply in-house cloud screening to Level-1 reflectances
  - Relies on a dedicated cloud-detection step to remove visible reflectance observations affected by clouds;
  - Observations do not contain any information to discriminate clouds from aerosols
  - Using cloud model information only could imply aliasing observed clouds into model aerosols

- Simultaneous assimilation of clouds and aerosols
  - Proxy towards a single MFASIS Cloud and Aerosol operator) : create an operator by combining simulated reflectances from a MFASIS-Cloud and a MFASIS-Aerosol runs
  - Major developments required on RTTOV side

- **Use Level-2 cloud-screened observations**
  - Involves the use of pre-processed Level-2 cloud-screened aerosol reflectances from instruments like MODIS (Aqua/Terra) or VIIRS (NOAA) on polar-orbiting satellites.
  - These products apply established cloud-screening algorithms, reducing cloud aliasing risks

Showcasing the importance of screening for MODIS cloud-cleared reflectances

8th May 2025

Departure maps (O-B) - All data

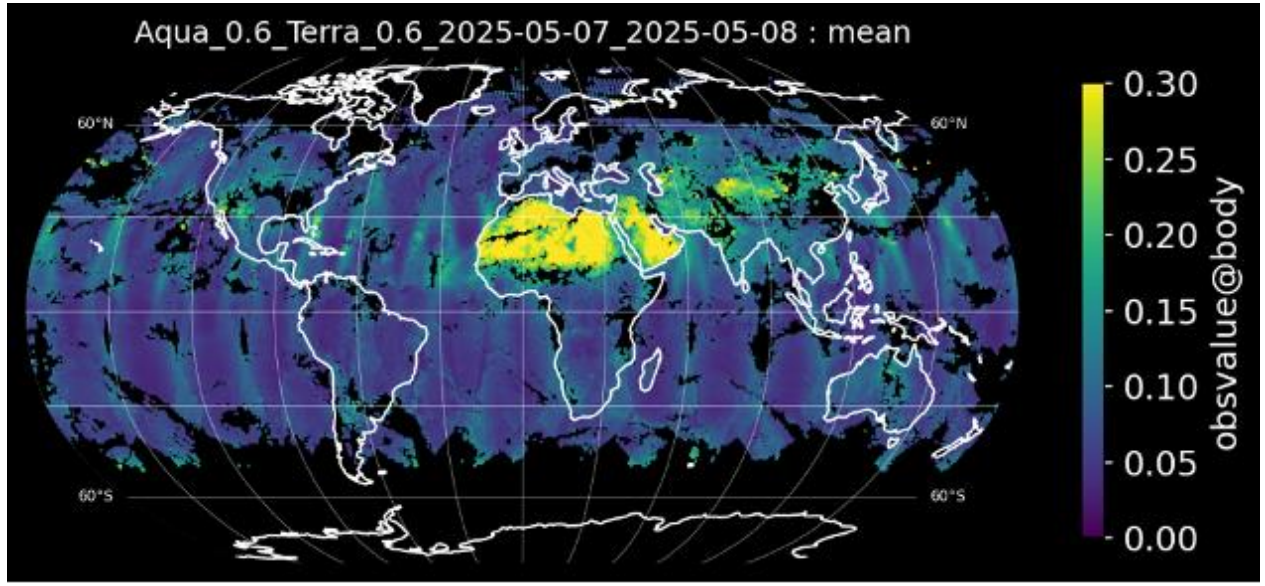

Ocean only
Sunglint
Sea ice
Large solar/satellite zenith angles
…

Departure maps (O-B) - Active data

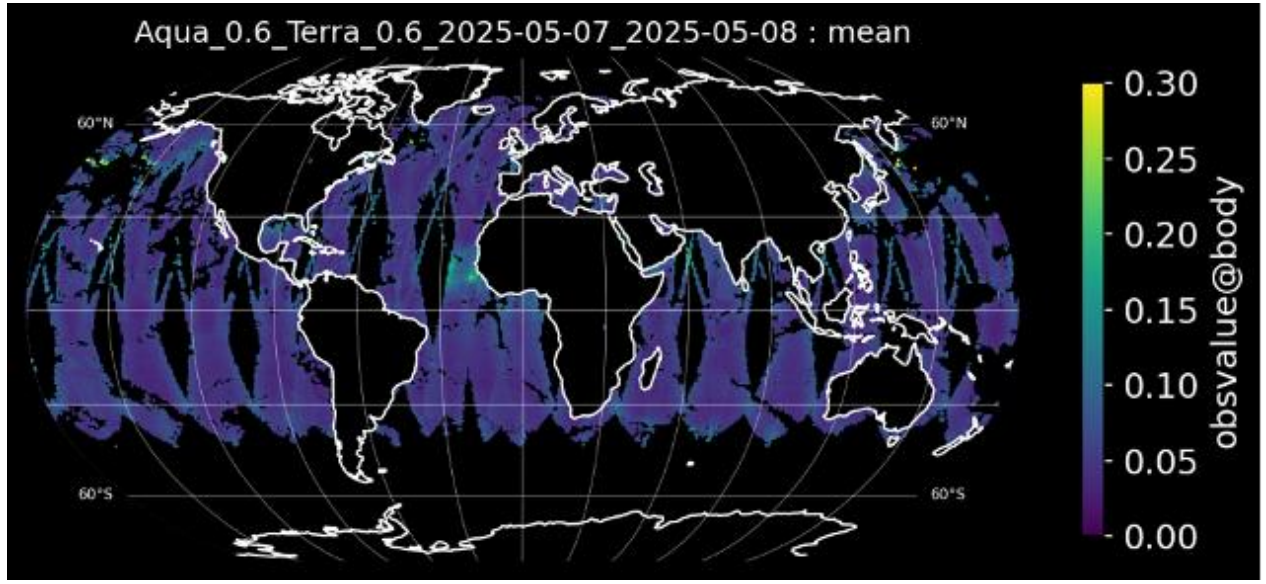

Showcasing the importance of screening for MODIS cloud-cleared reflectances

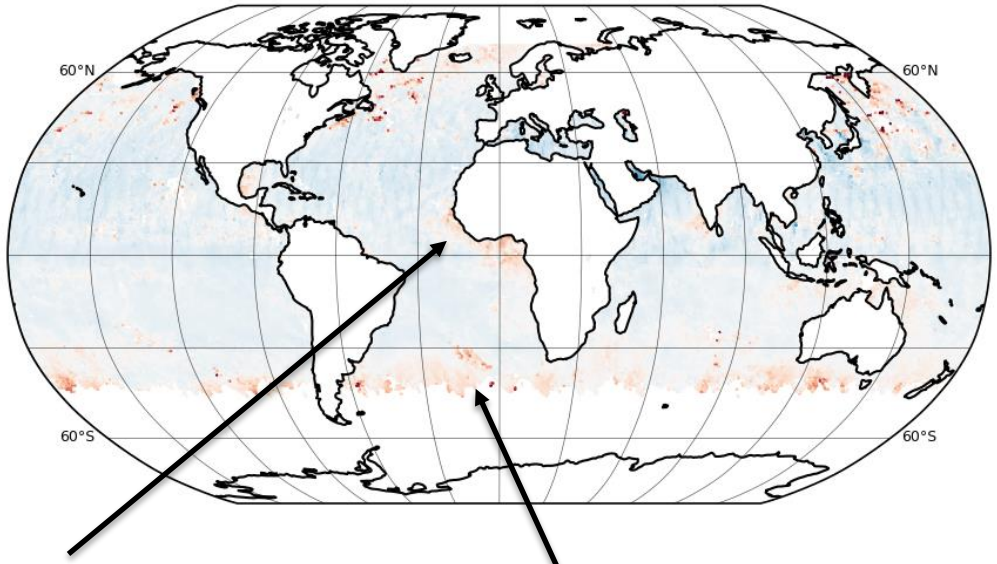

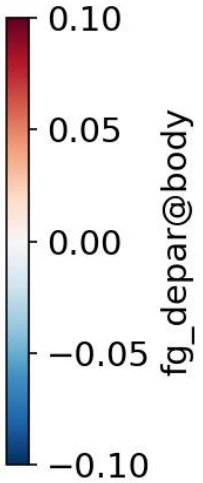

These results should be interpreted as proof of concept without drawing final scientific conclusions.

Note that MODIS MFASIS-Aerosol RT coefficients are not yet available (used here SEVIRI Meteosat-11 as a proxy)

There is a global small negative bias over ocean in the aerosol-clear scenes, together with a larger positive bias in the presence of aerosols.

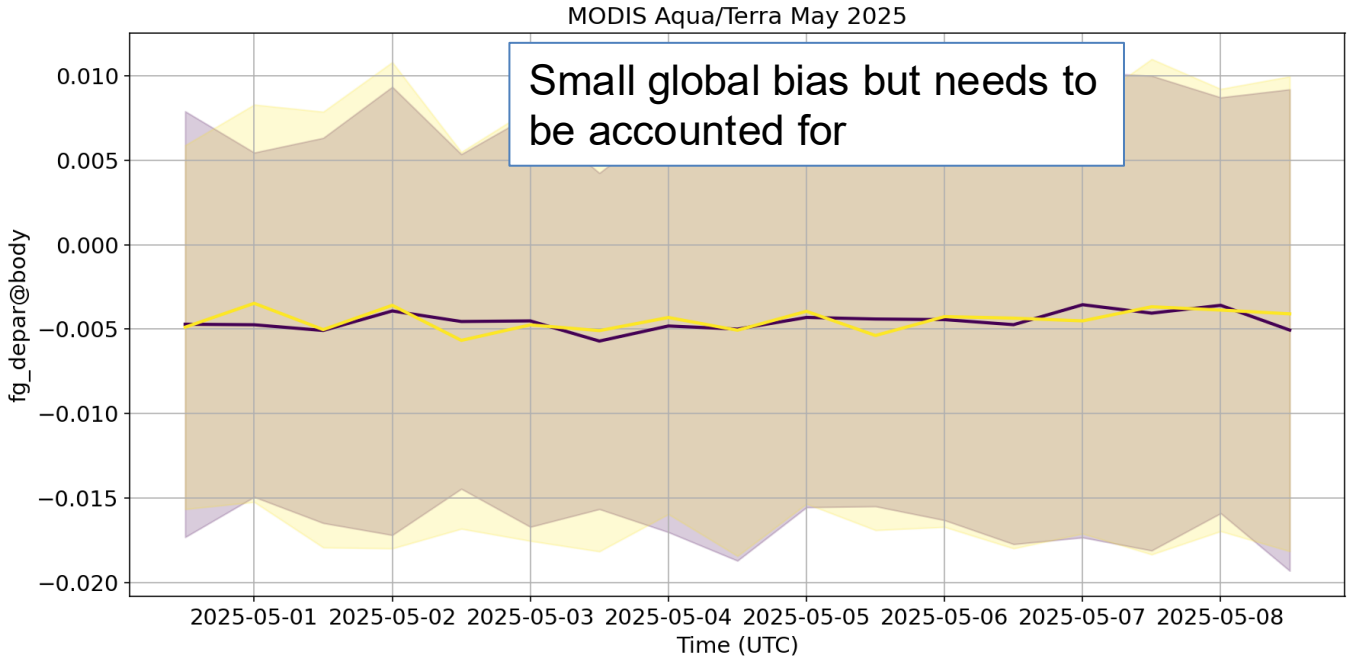

3. Cloud and aerosol visible reflectance assimilation: early results

- Cloud visible reflectance assimilation potential to improves low clouds in the IFS
- Case study of TC Sean
- Aerosol visible reflectance assimilation results in the IFS COMPO configuration
- Lighting assimilation

Case study: Low clouds over the Black Sea (23/04/25)

- Can visible reflectance assimilation improve low cloud representation in the IFS?

Visible reflectance (sea)

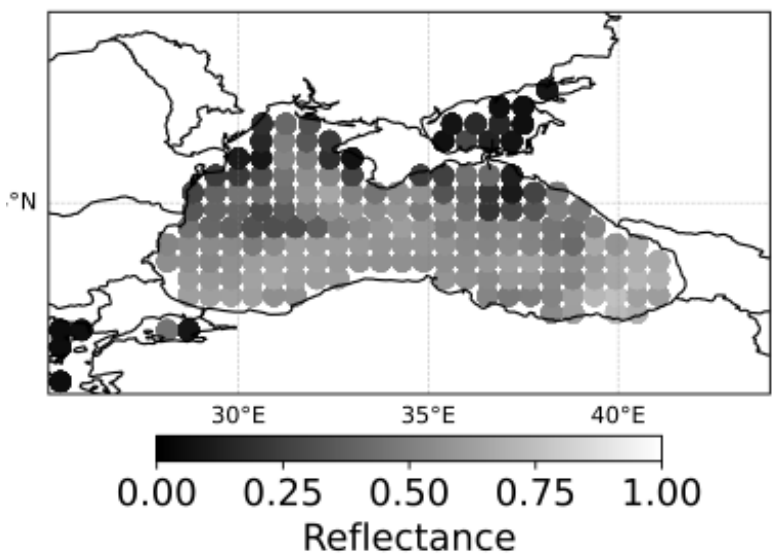

CTRL, OPS Analysis

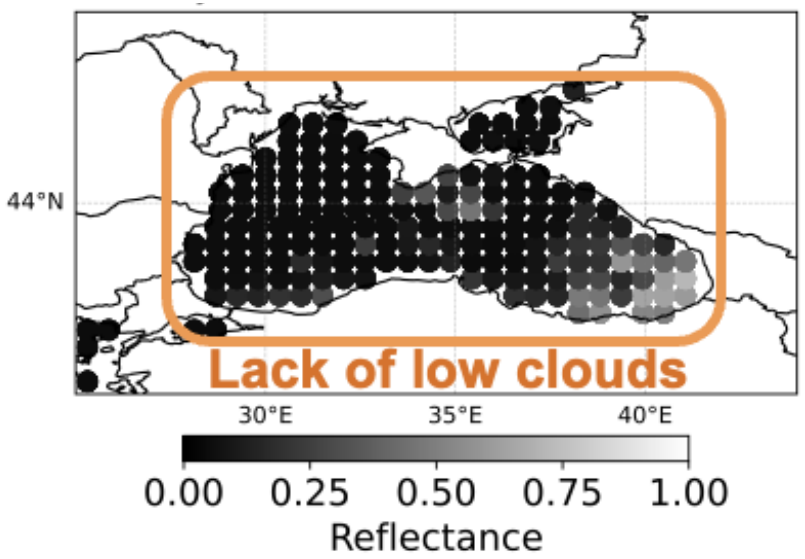

EXP, VIS Analysis

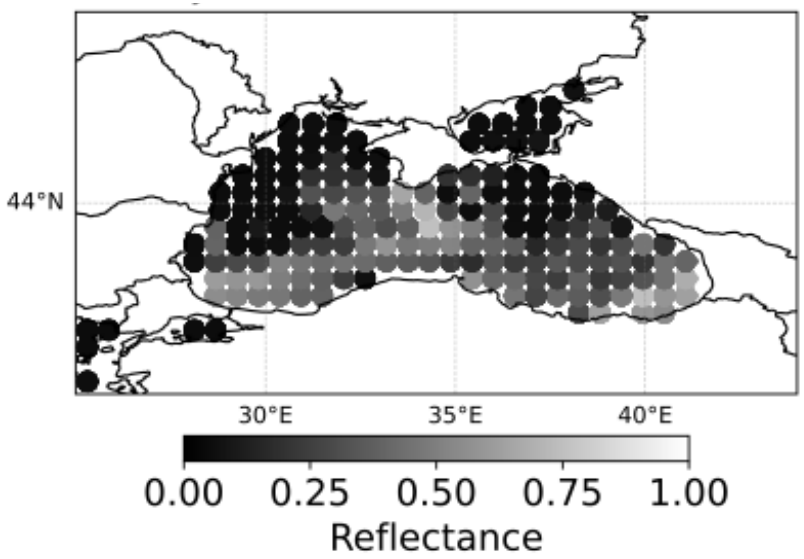

Case study: Low clouds over the Black Sea

- Can visible reflectance assimilation improve low cloud representation in the IFS?

Visible reflectance

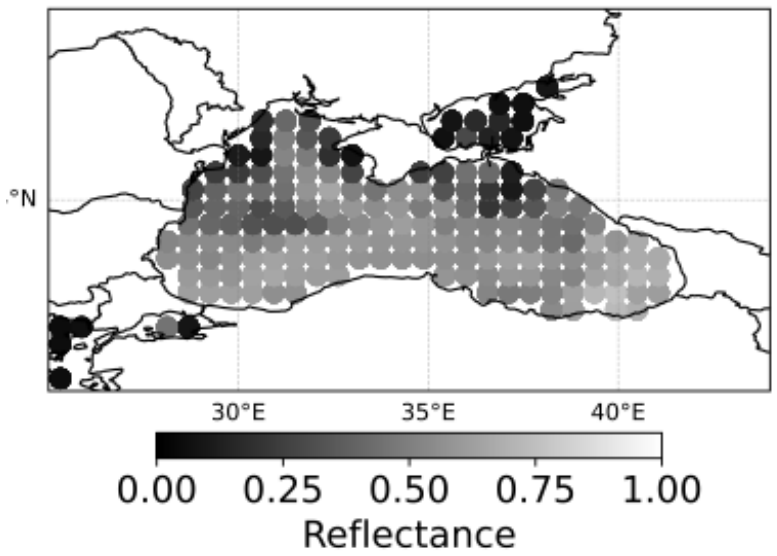

CTRL, OPS Analysis

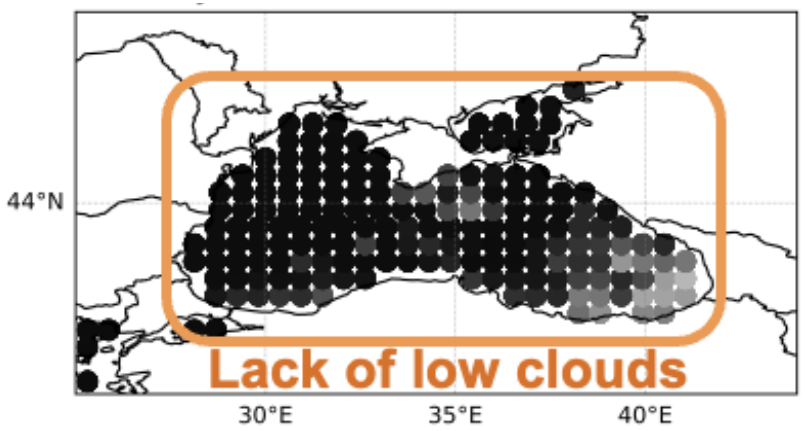

EXP, VIS Analysis

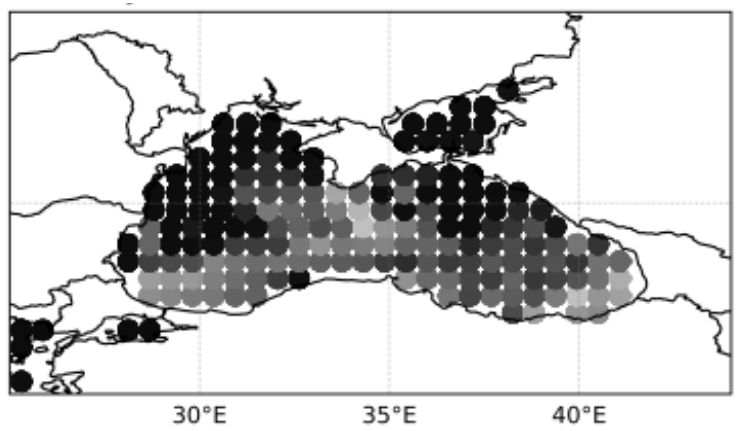

- Visible reflectance observations clearly "see" missing low clouds, enabling model correction.

- Improved departures after VIS assimilation (sea only)

CTRL, Analysis departure

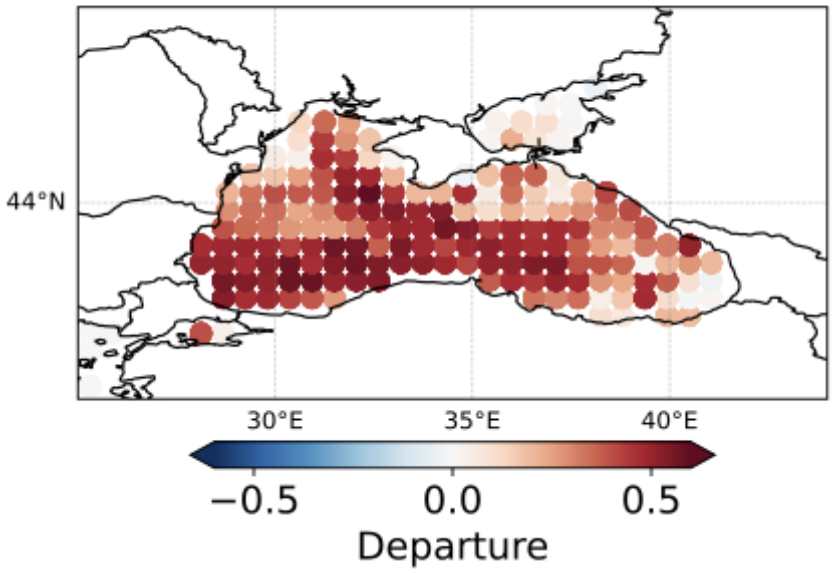

EXP, VIS Analysis departure

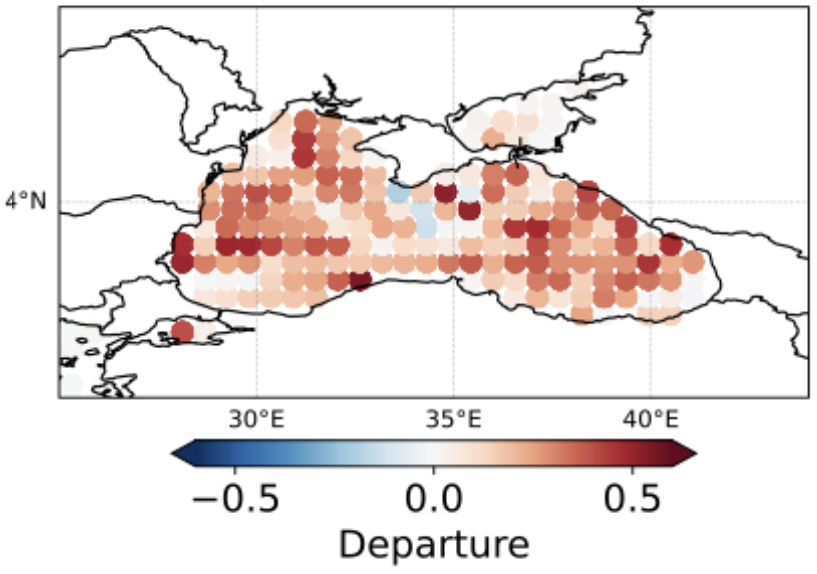

ECMWF

Case study: Low clouds over the Black Sea

Black Sea T/q mean differences (VIS DA – CTRL)

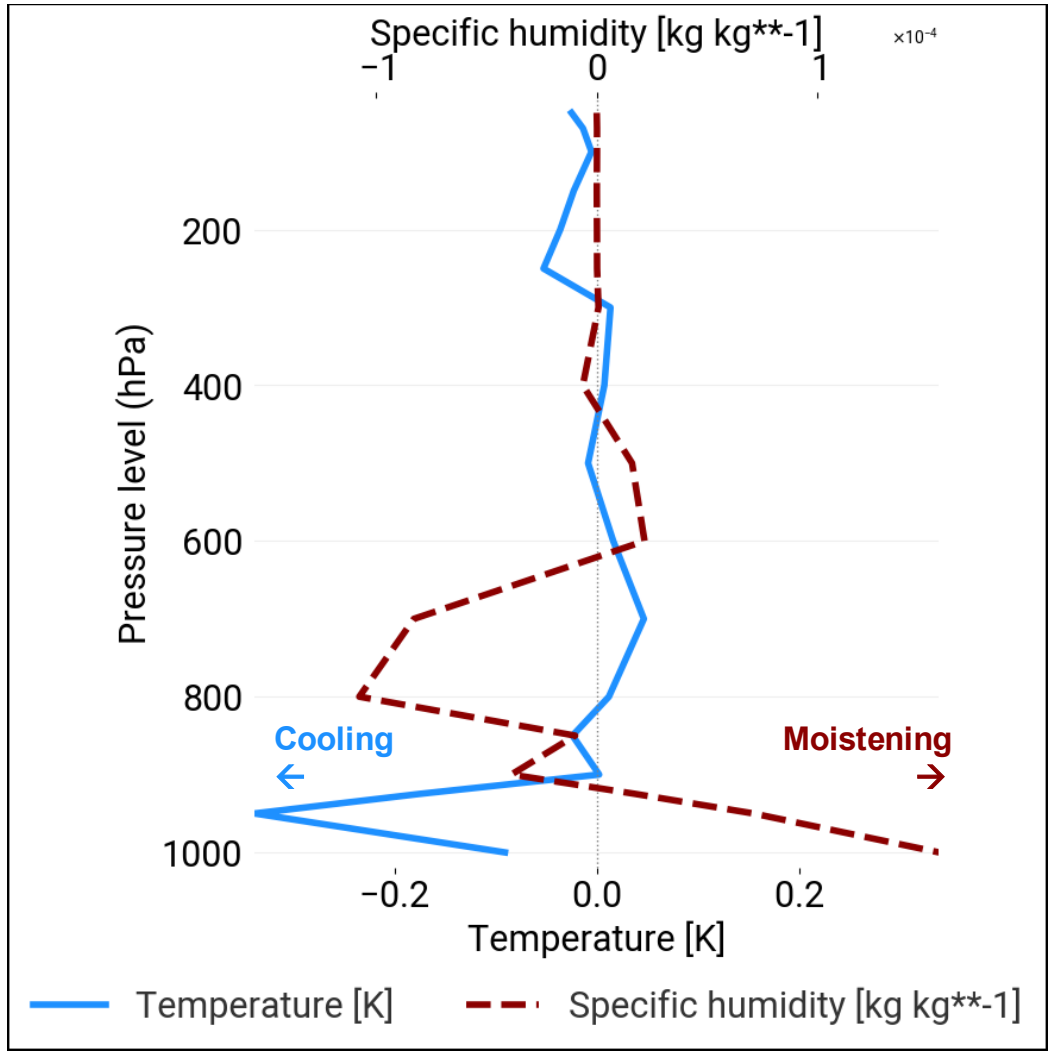

- Assimilating visible observations from OLCI and GEOS (sea-only) **increases the humidity** in the first kilometres, contributing to the formation and maintenance of the low clouds on top of the boundary layer.

Impact on short-range forecast fit to other observations

Period: 20 April - 20 May 2025
Exp = as OPS Control + VIS sea-only

Conventional wind

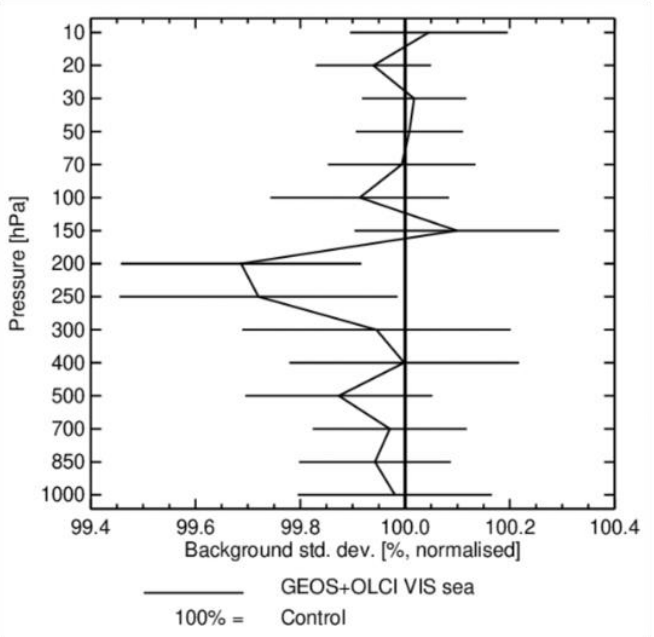

Aircraft-T

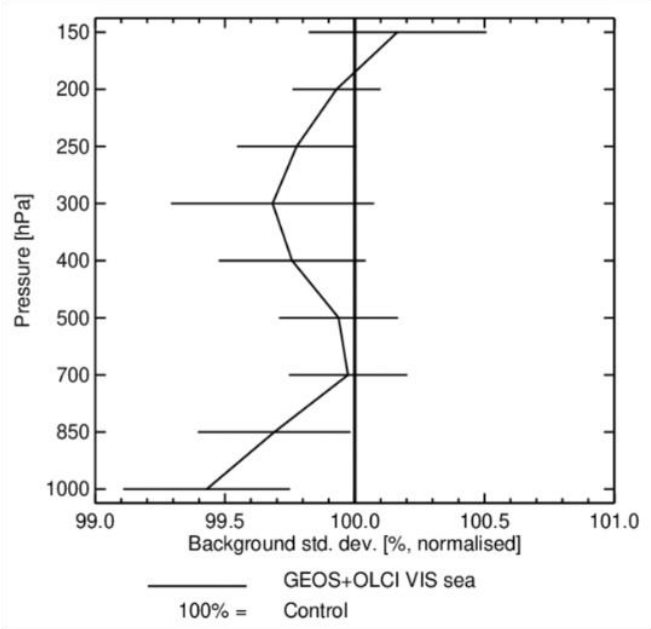

Aircraft-Q

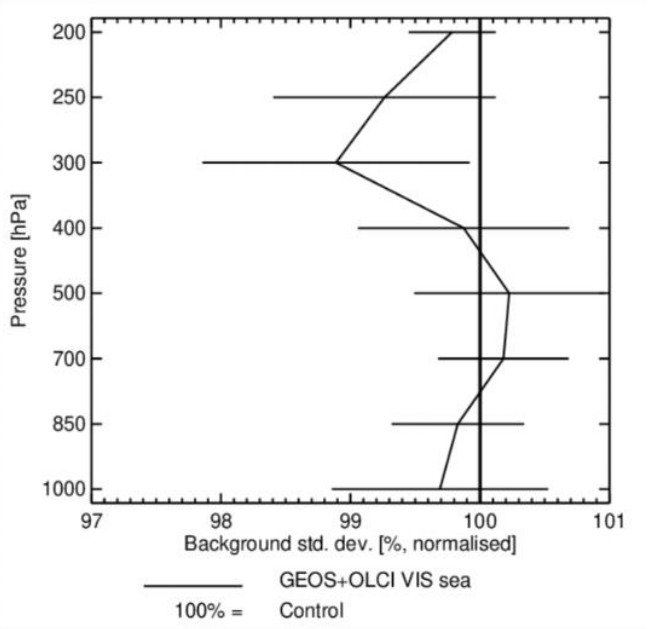

- Visible reflectances assimilation **provide information on temperature and humidity in cloudy areas** over the ocean which is consistent with the aircraft measurements.
- **First assimilation results are encouraging**, illustrating the potential of visible radiances to positively influence the analysis and the short-range forecast.
- Longer experiments covering at least two seasons will be needed for a full assessment of the medium-range impact.

Cloud visible assimilation substantially reduces reflectance departures

First guess departures

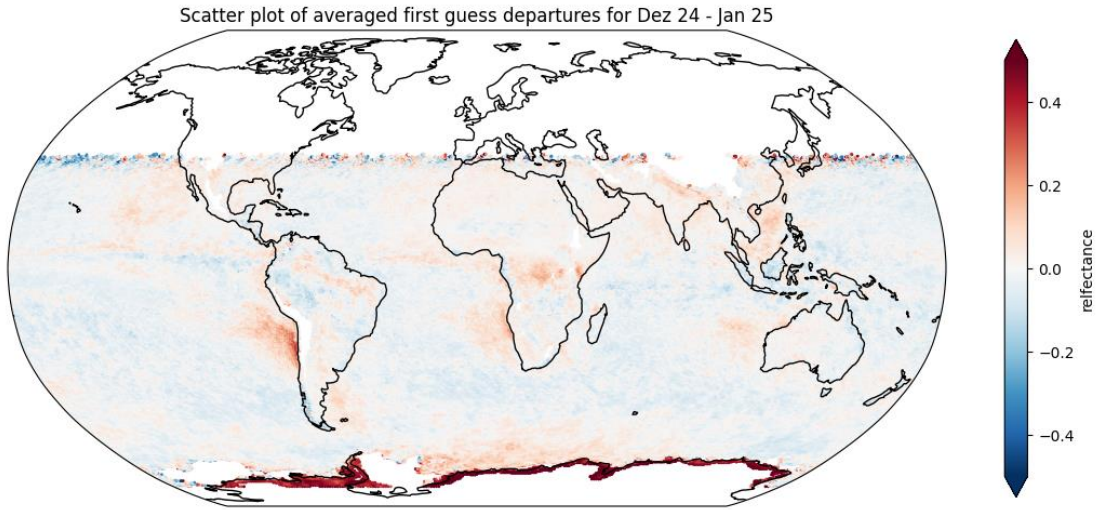

Absolute analysis increments

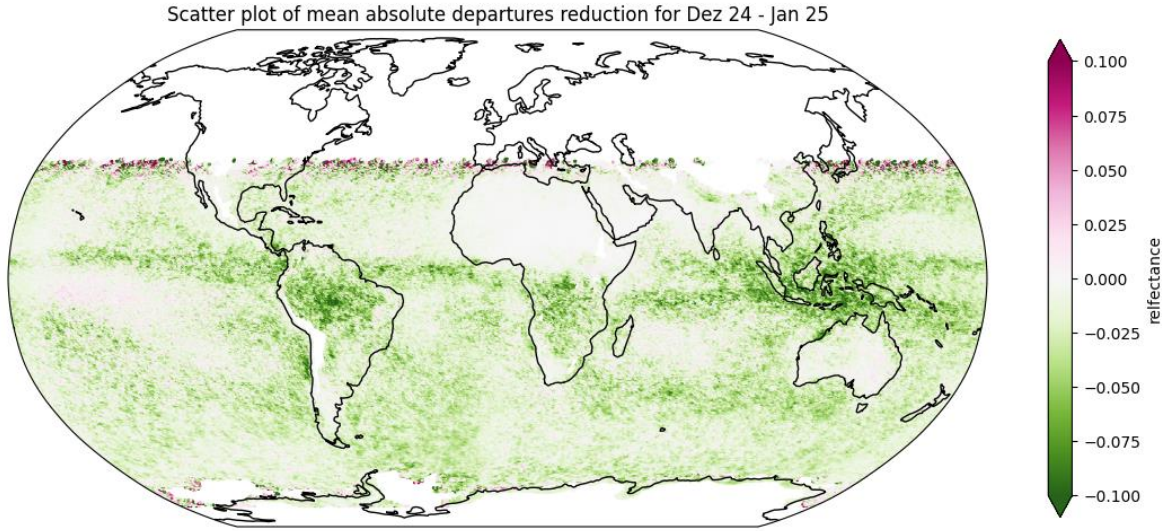

Analysis departures

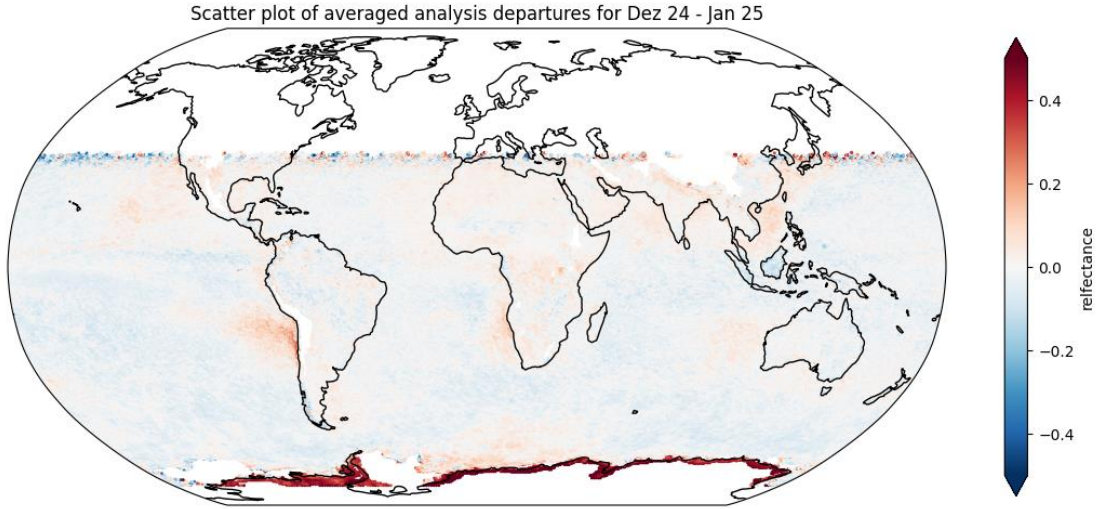

Monthly mean visible departure statistics

- **Dec 2024 – Jan 2025**
- Successful near-real time assimilation in IFS
- Assimilation, on average reduces differences between observation and model
- Largest improvements in the tropics and the Pacific Ocean near the Americas

What about the aerosols: Saharan Desert Dust event on 04/05/25

- Can aerosol visible reflectance assimilation enhance CAMS aerosol forecasts and atmospheric composition analyses?

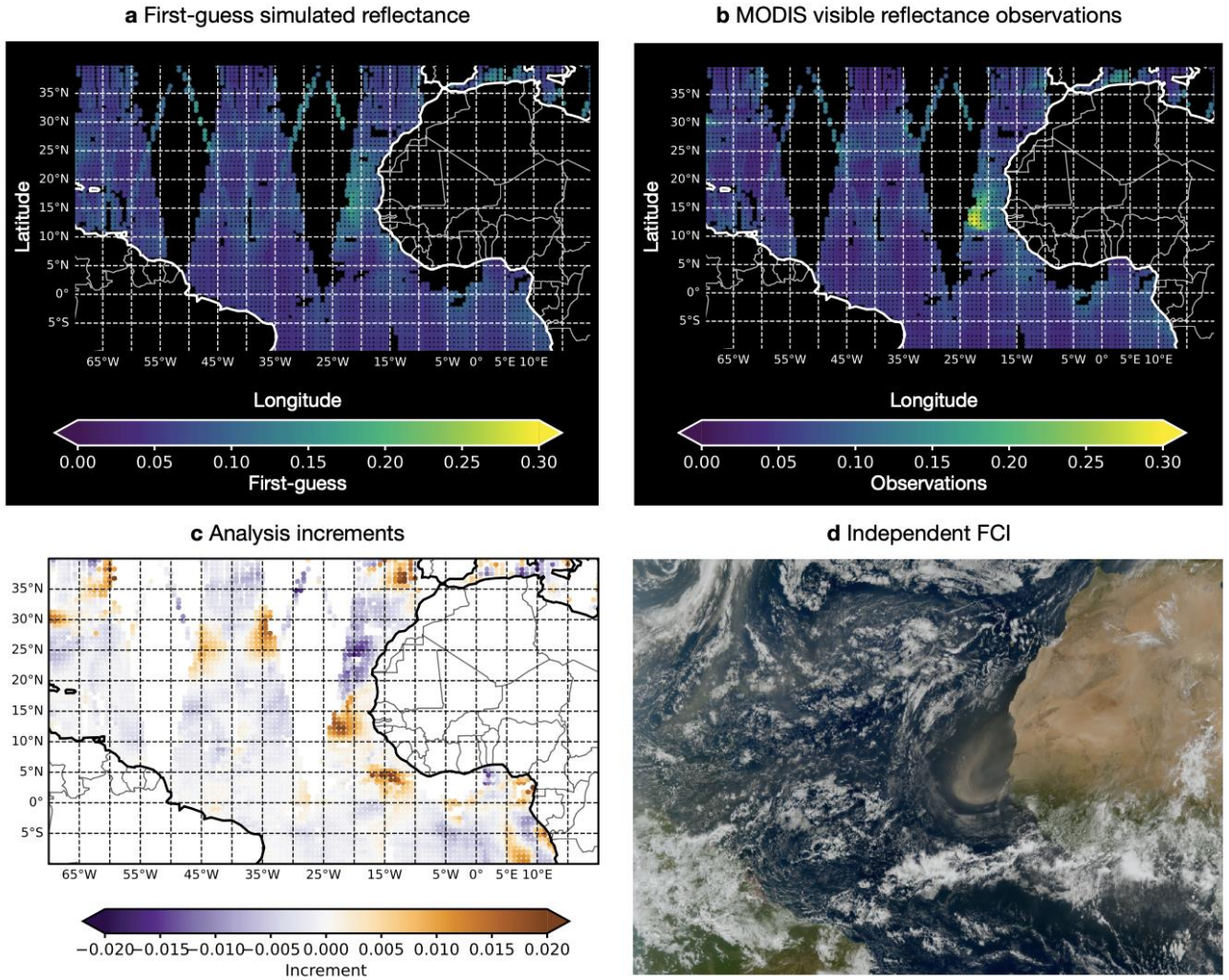

orange = increase AER
purple = decrease AER

- The model-simulated reflectances (top left) capture the aerosol signal in the same area as shown by MODIS observations (top right) but underestimate its intensity.
- Assimilation increases aerosol concentrations in the analysis (bottom left), enhancing the event representation.

https://www.eumetsat.int/saharan-dust-over-atlantic-ocean

Aerosol visible assimilation substantially reduces reflectance departures

First guess departures

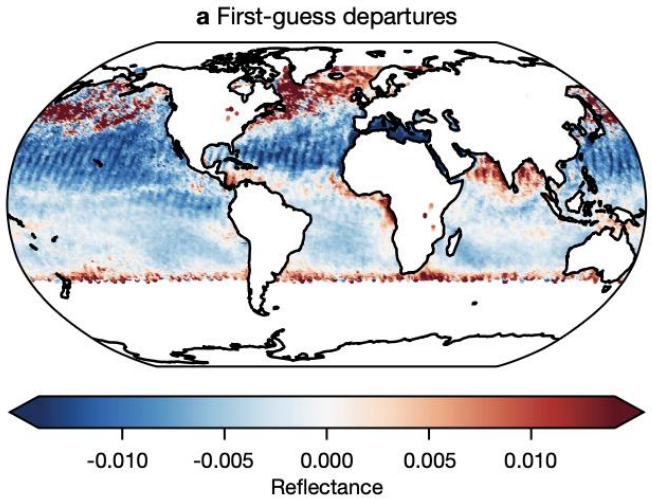

Analysis departures

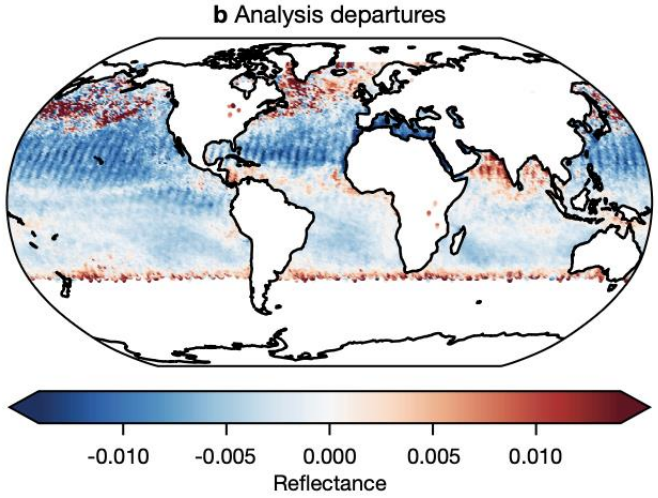

Absolute analysis increments

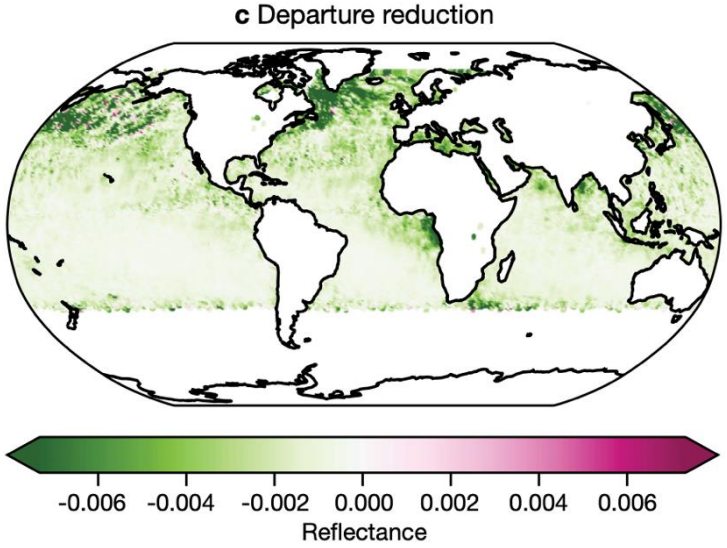

Monthly mean visible departure statistics

- **June 2025**
- Assimilation, on average reduces differences between observation and model
- A significant reduction can be seen in the Gulf of Guinea, north Atlantic and the W-coast of Africa.

Aerosol reflectance assimilation: sensitivity to error assumptions

obs_err = 0.05

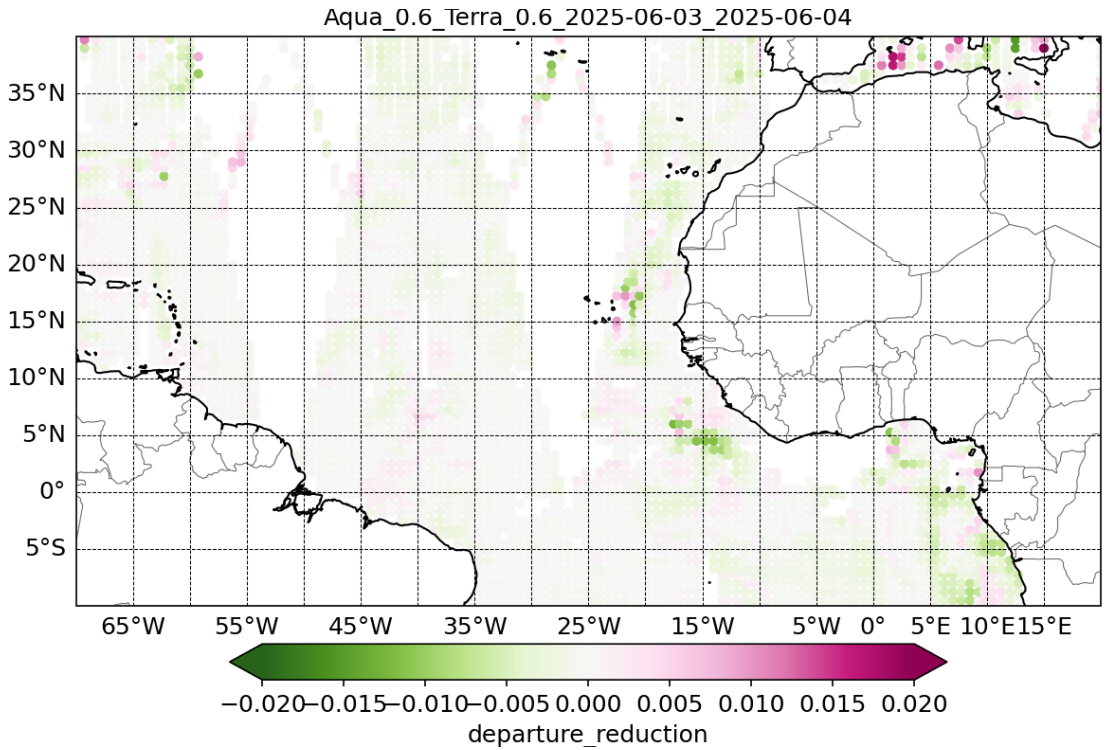

Departure Reduction (|dA|-|dB|)

obs_err = 0.015

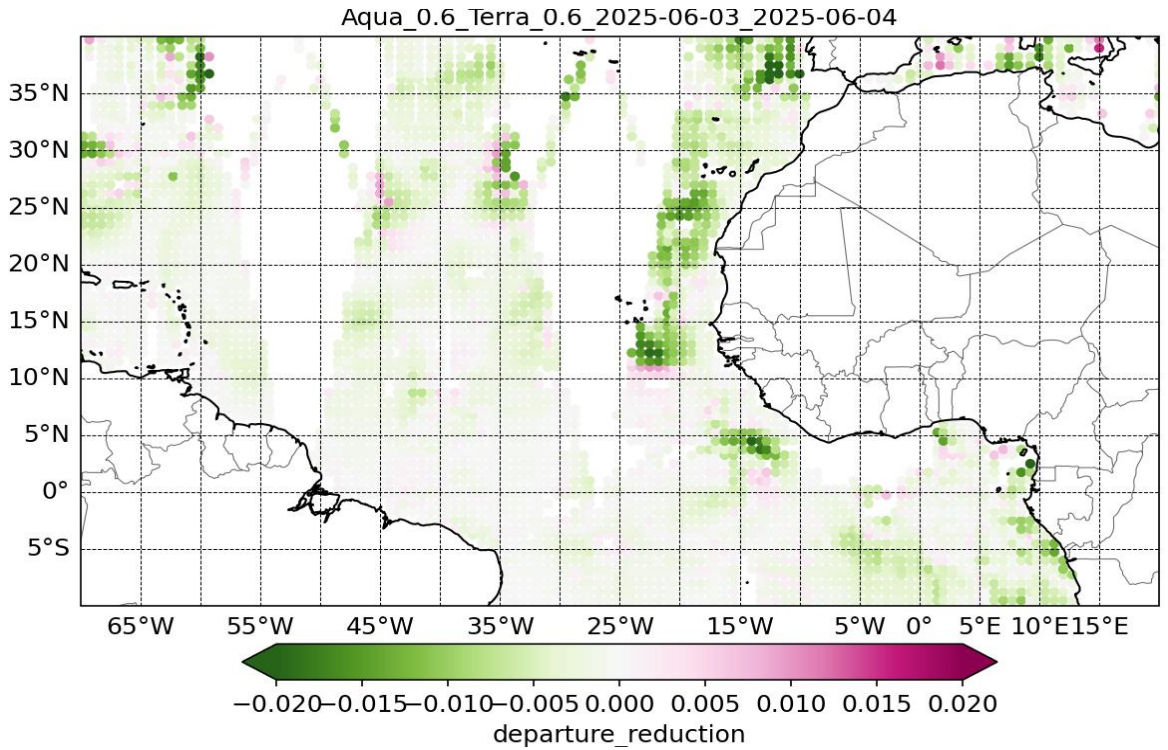

green = analysis closer to obs.
pink = analysis further from obs.

Comparison with independent Aerosol Optical Depth observations from AERONET

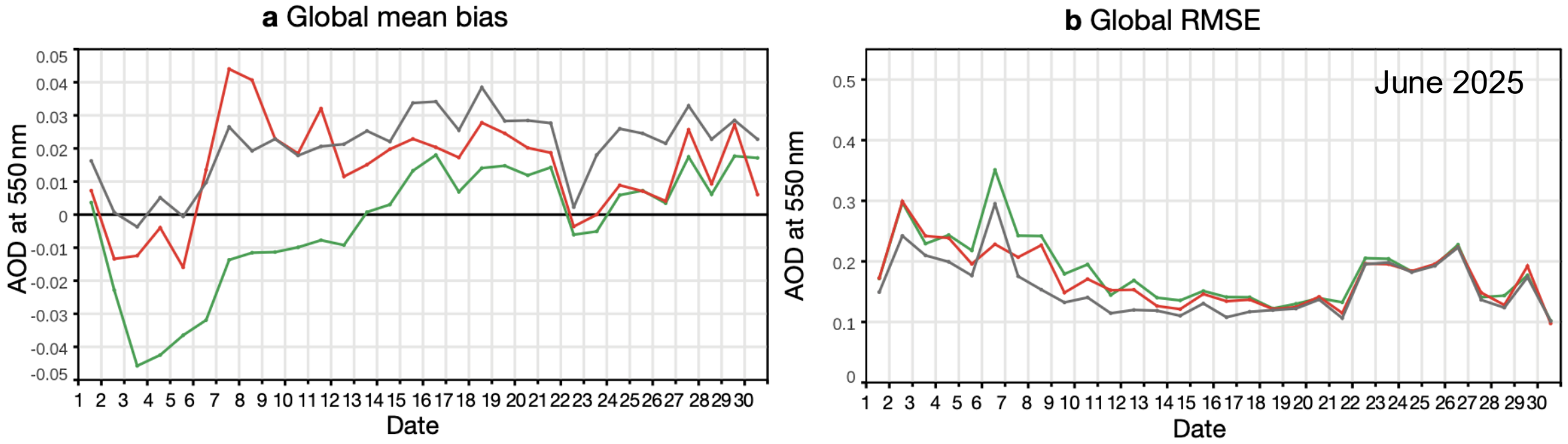

CTRL (without AOD or aerosol visible reflectance assimilation)
Aerosol visible reflectance assimilation (MODIS Level-2 cloud-screened 665 nm visible reflectances)
Baseline (with AOD assimilation as in CAMS operations)

- Aerosol visible reflectances assimilation exhibits a smaller bias compared to the AOD assimilation.
- The AOD assimilation experiment shows the smaller RMSE for most of the period.
- Visible reflectance assimilation shows, in general, lower RMSE than the control experiment, even improving upon the AOD experiment on specific days (e.g. on 6 June 2025).

4. Conclusions and outlook for visible radiance assimilation

Every Cloud has a Silver Lining (or some aerosols)

Outlook: All-sky visible monitoring and assimilation at ECMWF

- Advance operational exploitation of visible reflectance from multiple satellite sources targeting IFS, IFS-COMPO, future reanalyses, and cloud physics.
  - Scientific and technical infrastructure in place
  - Enable operational monitoring of visible reflectances for in IFS (upcoming operational cycle, Q2/2026)
  - Multi-satellite constellation: Sentinel 3A/B, MET-9/10/12, GOES-16/18/19, HIM-9

- Key challenges to obtain a more efficient data assimilation are being actively addressed (VarQC, observation error model, impact assessment …)

- Further information can be found in feature articles on visible assimilation, see ECMWF Newsletter No. 184 (clouds) and No. 186 (aerosols), https://www.ecmwf.int/en/publications/newsletters

5. Lighting assimilation

Toward the assimilation of lightning data from geostationary satellites

Observations: Lightning flashes (lon, lat, time; Level-2 product)
derived from optical signals in the 777.4-nm O2 band (peak emission from lightning). Continuous measurements.

Field of view of GOES GLM and MTG LI

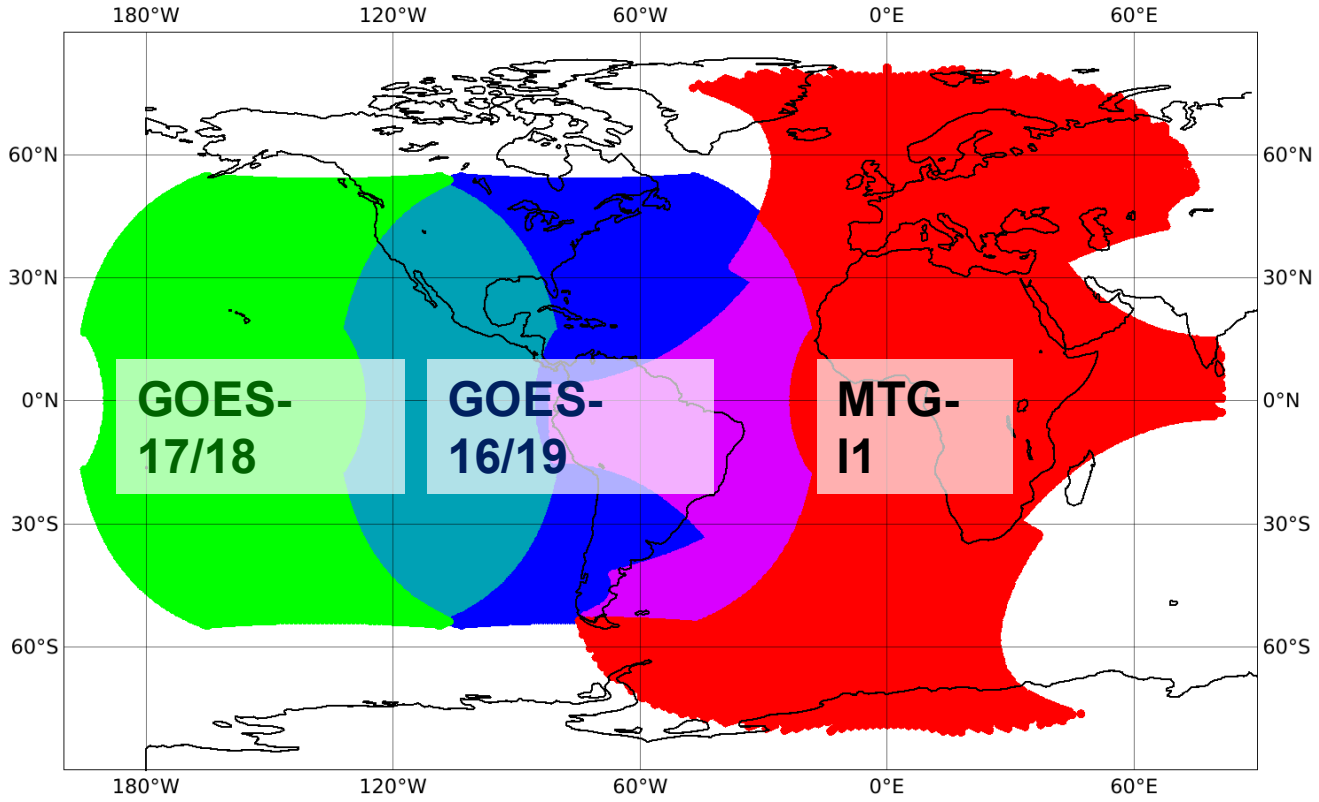

Credits: Philippe Lopez (ECMWF)

Quality Control of L2 flash data is needed (example of MTG LI)

Examples of transient cluster and line of spurious flashes (due to space debris crossing the FOV,

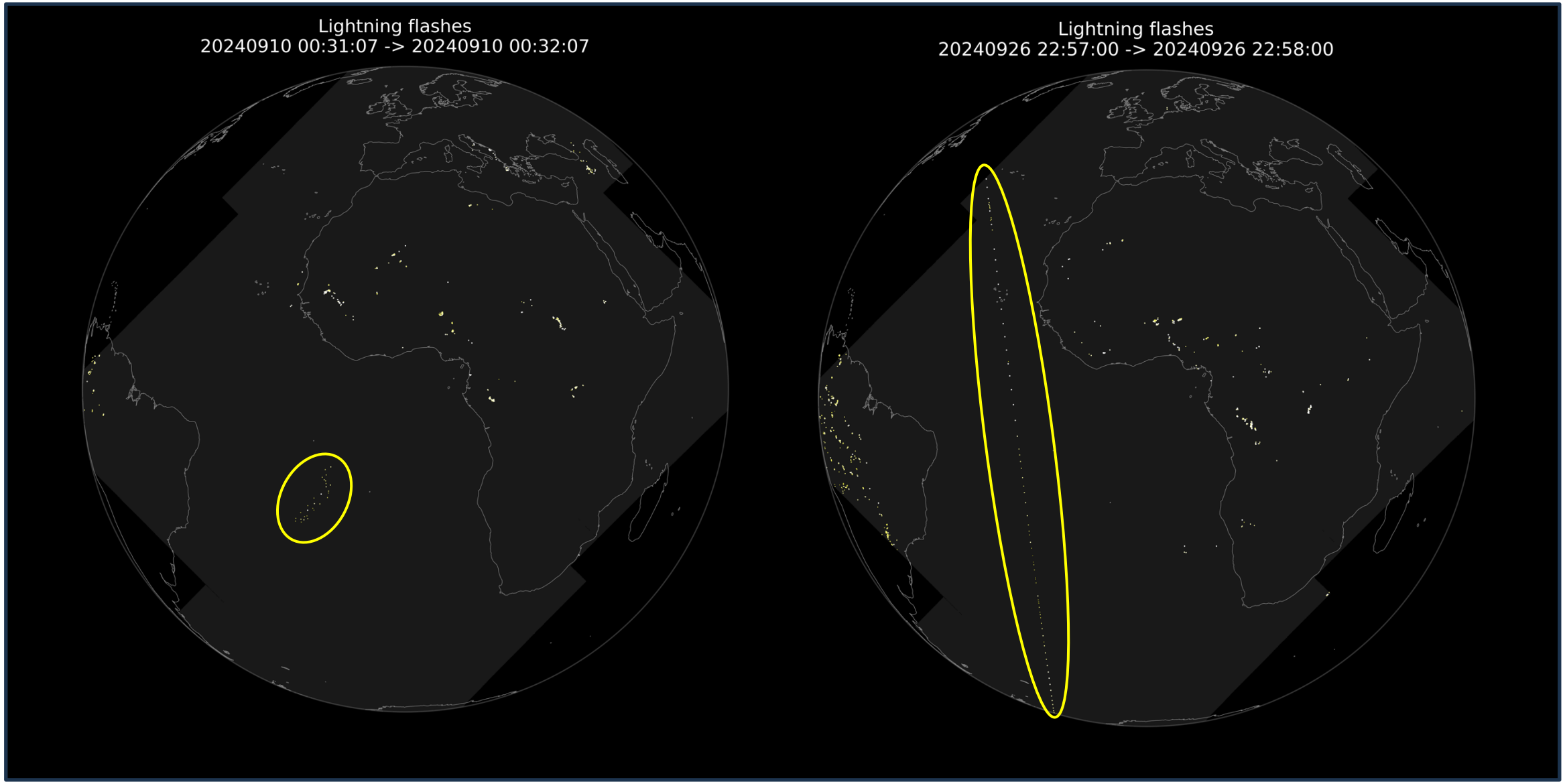

Assimilation of lightning flash densities at ECMWF

- Method:

  - Direct global 4D-Var DA (like all other observations already assimilated in ECMWF's IFS).
  - 6 or 12-hour assimilation window (every 6 or 12 hours, respectively).
  - In-house quality control of MTG LI and GOES GLM data is applied before assimilation.
  - Flash detection efficiency is assumed to vary between 70 and 88% (day/night).

- Quantity to be assimilated:

  - Observed lightning flash densities as derived from L2 flash data.
  - Simulated lightning flash densities from IFS using Lopez (2016).
  - Averaged over 6 hours (to reduce effects of non-linearities).
  - Log transform applied before assimilation (obs – model departures closer to Gaussian).

- Lightning monitoring/assimilation will be available in the forthcoming operational IFS version 50R1.

Lightning data assimilation: The asymmetry issue.

- Clear asymmetry in the performance of 4D-Var between cases with positive and negative obs−model lightning departures: it is much easier to reduce model lightning than to increase it, especially when the model background state is convection-free (and thus lightning-free).

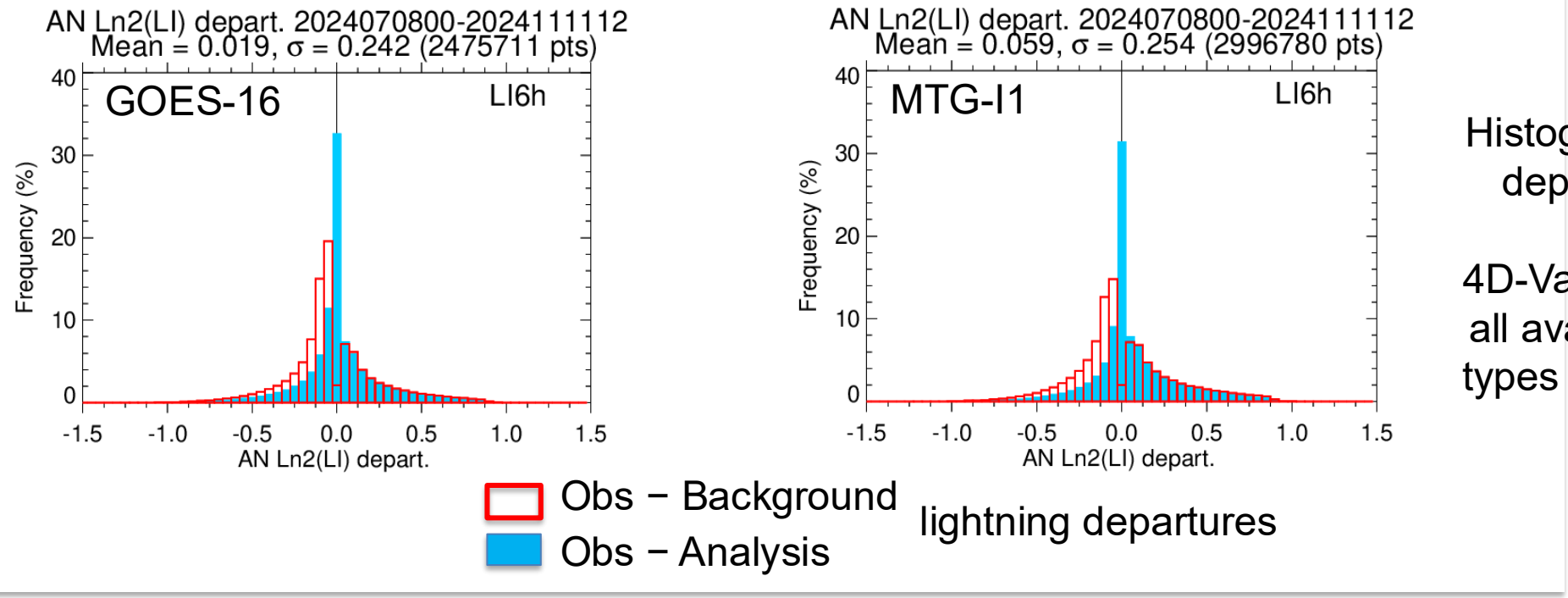

Histogram of obs−model departures from a 4-month 4D-Var experiment using all available observation types (28-km resolution).

- Reason for the asymmetry: When the model is lightning-free, the local gradient of the lightning observation operator to input T and q is zero → implemented an artificial sensitivity booster in TL and AD.

Geostationary satellite lightning assimilation: Preliminary experimentation

• 12h forecast RMSE differences due to 4D-Var assimilation of GOES-16/18 GLM & MTG-I1 LI (8 Jul – 17

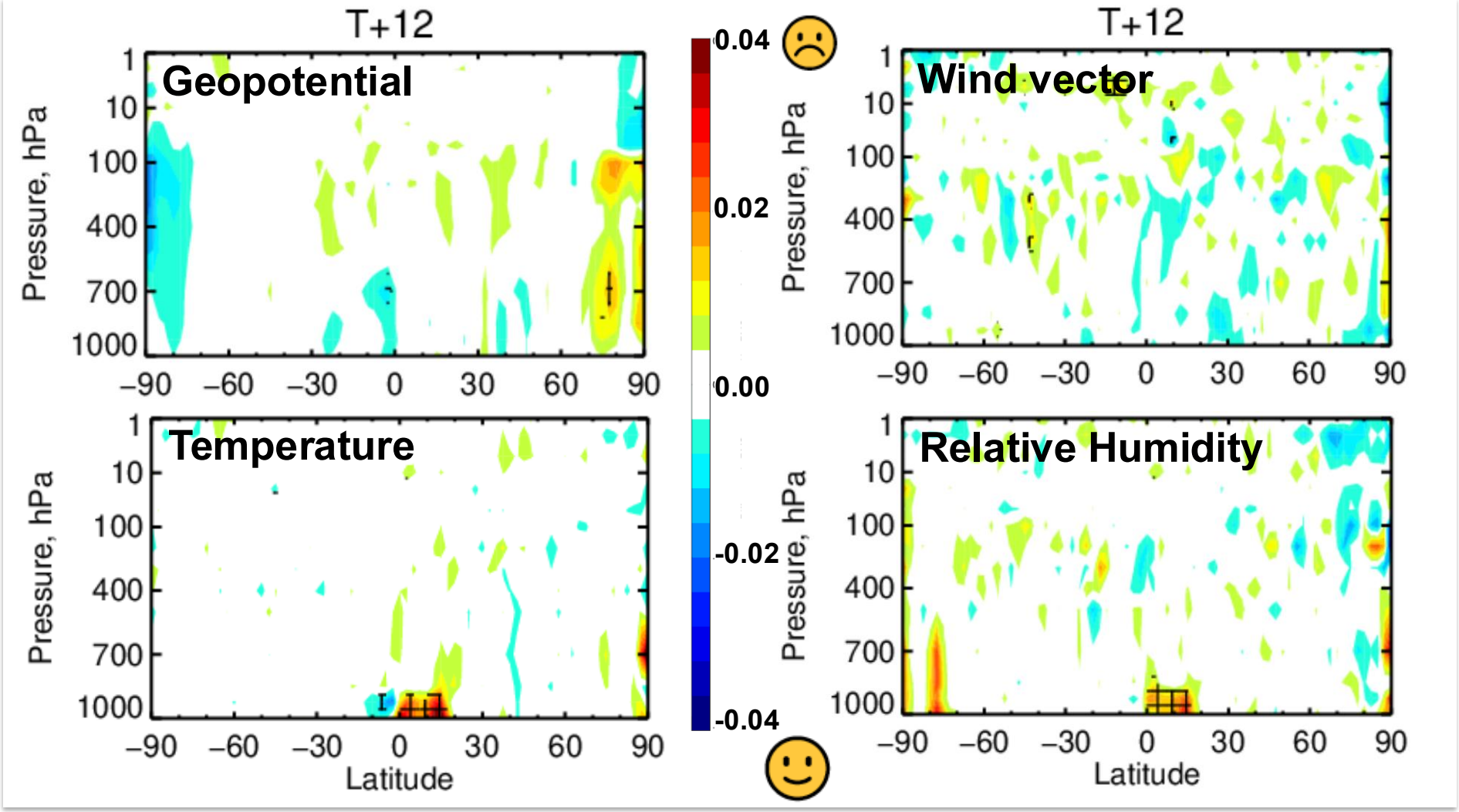

4D-Var using all available obs types (28-km resol).

Zonal mean cross-sections of impact on RMSE.

→ No sign of major degradation; room for improvement near surface in the Tropics (Amazon & Africa).

Summary & Plans

- Monitoring of lightning data from MTG LI and GOES GLM planned in 2026 (IFS CY50R1).

- Ongoing work to maximize impact on weather prediction:
  - Tuning of the lightning sensitivity booster (zero-gradient issue in 4D-Var);
  - Adjusting error statistics (esp. for observations);
  - Optimizing the averaging period applied to lightning flash densities (6, 3 or 1 hour?);
  - Assessing the relevance of including a bias correction.

- Longer term:
  - Prepare for future lightning instruments on board MTG-I2 (2026) and MTG-I3 (2032?).

References / 1

- **Baur, F., L. Scheck, C. Stumpf, C. Köpken-Watts & R. Potthast** (2023) A neural-network-based method for generating synthetic 1.6 µm near-infrared satellite images. *Atmospheric Measurement Techniques*, 16, 5305–5326. https://doi.org/10.5194/amt-16-5305-2023

- **Benedetti, A., S. Quesada-Ruiz, J. Letertre-Danczak, M. Matricardi & G. Thomas** (2020) Progress towards assimilating visible radiances. *ECMWF Newsletter* No. 162. https://www.ecmwf.int/en/newsletter/162/news/progress-towards-assimilating-visible-radiances

- **EUMETSAT** (2025) Satellite Application Facility for Numerical Weather Prediction (NWP SAF) RTTOV v14. https://nwp-saf.eumetsat.int/site/software/rttov/rttov-v14/

- **Geer, A. J. & P. Bauer** (2011) Observation errors in all-sky data assimilation. *Quarterly Journal of the Royal Meteorological Society*, 137, 2024–2037. https://doi.org/10.1002/qj.830

- **Necker, T., A. Benedetti, S. Quesada Ruiz & C. Lupu** (2025) Assimilation of Cloudy Visible Radiances (CloVIS-2): Further steps towards establishing a Cloud Analysis in the Visible. Final Report v0.3, ECMWF (available from ECMWF).

- **Necker, T., Lupu, C., Benedetti, A., & Quesada-Ruiz, S.** (2025, March 18) Seeing the Unseen – Progress towards all-sky visible reflectances monitoring and assimilation at ECMWF. *Meeting on Perspectives on Visible Radiance Exploitation in Numerical Weather Prediction*, ESA-ESRIN, Frascati, Italy. Zenodo. https://doi.org/10.5281/zenodo.15045412

References / 2

- **Necker, T., Quesada-Ruiz, S., Lupu, C., Firat, V., & Benedetti, A.** (2025) Progress towards assimilating cloud visible reflectances at ECMWF. *Workshop on Data Assimilation: Initial Conditions and Beyond*, Bonn, Germany. Zenodo. https://doi.org/10.5281/zenodo.15211148

- **Scheck, L., M. Weissmann & L. Bach** (2020) Assimilating visible satellite images for convective-scale numerical weather prediction: A case-study. *Quarterly Journal of the Royal Meteorological Society*, 146, 3165–3186. https://doi.org/10.1002/qj.3840

- **Scheck, L.** (2021) A neural network based forward operator for visible satellite images and its adjoint. *Journal of Quantitative Spectroscopy & Radiative Transfer*, 274, 107841. https://doi.org/10.1016/j.jqsrt.2021.107841

- **Steele, L., A. Benedetti, M. Matricardi, A. Geer & P. Lean** (2022) Initial results of monitoring cloudy visible radiances. *ECMWF Newsletter* No. 171, 7–8. https://www.ecmwf.int/en/newsletter/171/news/initial-results-monitoring-cloudy-visible-radiances